ONR-URI Composites Program
Technical Report No. 13

UIUC-NCCMR-89-#0013

CHARACTERIZATION STUDIES OF FLUORINATED EPOXY RESINS: NAVAL EXPERIMENTAL RESIN C8/1SA AS A STRUCTURAL MATERIAL AND FOR USE IN BLENDS AND COMPOSITES*

T. E. Twardowski** and P. H. Geil***

June 1, 1989

National Center for Composite Material Research
at University of Illinois, Urbana - Champaign
A DoD University Research Initiatives Center funded by the
Office of Naval Research, Arlington, VA

---

* This report is the M.S. thesis of T. E. Twardowski. Three publications (notes) are being prepared for publication based on its contents, i.e. matrix characterization, composite characterization and use in blends.

** ONR-URI Fellow, Polymer Division, Department of Material Science and Engineering

*** Professor, Polymer Division, Department of Material Science and Engineering

TABLE OF CONTENTS

1. INTRODUCTION

Epoxy thermosets are currently the material of choice for high performance composite materials. They have high modulus, low weight, excellent adhesion to the filler component, and high dimensional and thermal stability as well as processing characteristics much more tractable than thermoplastics. Unfortunately, epoxies are often attacked by environmental elements, especially water, resulting in a degradation of properties[a]. As such, modification of epoxies to improve their environmental resistance is a valuable consideration. Epoxy resins incorporating large fluorine contents have met this challenge, showing low contact angle, low moisture uptake and improved flame resistance[5]. What remains is the need to investigate the suitability of such resins for use in structural materials.

1.1 Background

Griffith and Field[5] have synthesized many fluorine containing epoxy resins, the most successful types of compound having the form:

[a]such as the glass transition[1,2] and adhesion with substrates and reinforcements[3,4].

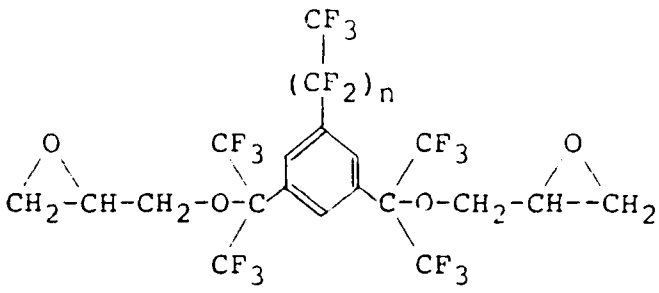

where the resin is named for the number of carbons in the side chain, which can vary from 0 to 8. These resins are miscible with silicone amine curing agents of the general form:

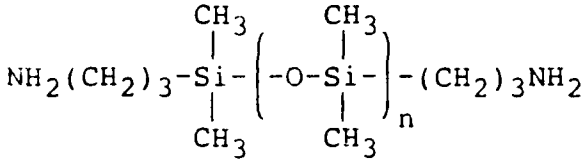

which are designated [n]SA, 1SA being the type most readily available. Griffith[6] has also synthesized fluoroanhydride curing agents to further boost the fluorine content of the available resins. One of the most commonly studied has the form:

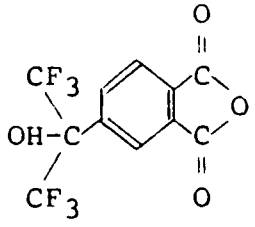

and has been designated FA. The reaction kinetics of the fluoroepoxy resin systems have been characterized by Griffith, Reines and O'Rear[7].

Hunston, Griffith and Bowers[8] examined the surface properties of the fluoroepoxies. They found a high coefficient of friction, in contrast with Teflon, and a low

critical surface tension. In addition, the low surface tension of the resins made them compatable with Teflon and Barrier Film[b] powders, resulting in materials with low friction and surface energy, and with strong barrier properties and toughness, respectively, upon curing.

Shaw, Tod and Griffith[9] have characterized the water uptake behavior as well as some of the mechanical properties of the material. They found remarkable resistance to moisture even at hot wet temperatures of 60°C (Table 1). Shaw[10] has since continued his work on the fracture and dynamic mechanical properties of various resin systems. His results show moderate strength but low glass transitions, especially in the SA cured systems (Table 2, Figure 1). It has been suggested that the increase in water uptake in the C8/FA resin is due to residual curing agent reactivity or incomplete crosslinking.

These materials can be used in many applications from aquatic to automotive. As mentioned previously, the resins make good suspensions with Teflon powder and Barrier Film, and coatings utilizing these properties are currently being used[8]. Other proposed uses include[5,6]: structural materials, high friction and hydrophobic coatings, dental prosthetics, flame resistant plastics, solid propellent matrices, optical cements, laser window sealants, and fouling release coatings. The resins are currently being

[b]1H,1H-pentadecafluorooctyl methacrylate.

manufactured in pilot plant quantities by Allied Chemical Company.

1.2 Methods

Differential Scanning Calorimetry

There is a wealth of information that can be gathered on thermosetting materials using the DSC. For example, the glass transition can be tracked. As a material is postcured its T_g will gradually shift to higher temperatures, eventually reaching the postcuring temperature. A material which is not fully cured will exhibit an exothermically sloped baseline which is known as the residual exotherm. Degradation is reflected by a downward shift in T_g.[11]

Thermally Stimulated Current

The thermally stimulated current method (TSC) is a high resolution method for tracing the behavior of dielectrically active transitions. The technique consists of applying a high voltage across the samples at a selected temperature. This aligns any dipoles in the sample that are mobile at this temperature; the sample can then be quenched with the field still applied to "freeze" in the orientation. If the sample is then short circuited across an ammeter and heated, a current can be measured as the dipoles relax. This technique has been used to characterize the low temperature

relaxations of DGEBA type epoxy resins by Pangrle, Wu and Geil[12].

Pangrle, et. al, found several relaxations, labeled γ, β, β_{OH}, β' and β'' in order of increasing temperature. These peaks were attributed to the motions of diphenyl propane, crosslinks in less densely crosslinked regions, hydroxyether linkages, crosslinks in more densely crosslinked regions and an interaction with water, respectively (Figure 2).

TSC can also be used to study the higher temperature (α) relaxations due to the glass transition.[13] Often, there is a ρ peak asscciated with and 30°C higher than T_g; this peak is attributed to the migration of trapped, injected space charges.

Single Fiber Tests

The interfacial strength of a matrix to a fiber can be measured using single fibers imbedded in a dogbone matrix (Figure 3). Such methods have been employed by Bascom and Jensen[14] and by Drzal[15]. They involve pulling a sample such as that illustrated in Figure 3 in tension. The fiber breaks into lengths of a critical minimum value (ℓ_c). As a stress is applied to the sample, it is transmitted to the fiber by the fiber matrix interface. When the stress field exceeds the strength of the fiber, the fiber will break. The distance between breaks corresponds to twice the distance required for the interface to transmit the maximum stress the fiber can carry, due to the constraints requiring

the stress to be zero at either fiber end. Statistical variations in fiber strength and matrix adhesion and interfacial transfer strength will cause some fluctuations in the values of ℓ_c as measured in a real situation, so an average of many such lengths is often required. The critical length is related to the interfacial shear stress. One such expression reported is:

$$\tau_c = \frac{\sigma_c d}{2\ell_c}$$

where τ_c is the shear stress, σ_c is the ultimate strength of the fiber and d is the fiber diameter[15].

1.3 Objectives

Choice of Materials

For reasons including the excellent hydrophobicity and ease of curing the material, the C8/1SA resin system was studied. Griffith recommended the curing conditions suggested by Shaw[6]: a curing schedule of 16 hours at room temperature followed by a postcure of three hours at 120°C, hereafter defined as fully postcured. The probable chemical form of the crosslinks are detailed in Figure 4. The number of tests conducted were somewhat limited by resin supply.

Characterization of the Neat Resin

The first step in the determination of the viability of the fluoroepoxy resin as a structural material was the

characterization of the neat resin. The behavior of the relaxations and transitions as a function of cure, as well as physical aging, swelling and the temperature dependence of the tensile modulus were evaluated.

Properties of an Epon 828/C8/1SA Blend

The C8 resin alone is a relatively weak material. One method of obtaining a material with the required strengths and hydrophobicity is blending resins with the desired properties. A blend of 10% by weight fluoroepoxy with Epon 828, cured with the same silicone amine curing agents with which the fluoroepoxies are cured, was investigated. The tensile modulus and processing dependent morphology of this material were studied.

Properties of a C8/1SA Carbon Fiber Composite Material

Use of the C8/1SA resin system as a matrix in carbon fiber composite materials is also a viable method for the improvement of properties. Tensile modulus, fracture morphology and adhesion strength were investigated for a C8/1SA resin matrix with a carbon fiber continuous phase.

Fiber and Interlaminar Coatings

The primary mode of environmental attack in composite structures is along fibers and at laminated ply interfaces. The hydrophobicity of the fluoroepoxy would be most effective if present at these interfaces. The interface strength

of a carbon fiber coated with C8/1SA in an Epon 828/1SA matrix, as well as the adhesion of two Epon 8280/V40 plys glued together with C8/1SA was investigated.

Table 1. Maximum water uptake for fluoroepoxies at various temperatures[9].

Formulation	Maximum Water Uptake (%)			
	20 °C	40 °C	60 °C	90 °C
C_0/1SA	0.69	0.85	1.07	35.72
C_6/1SA	0.27	0.45	0.43	2.04*
C_8/1SA	0.26	0.37	0.37	0.62
C_6/7.5SA	0.72	3.05	3.79	27.99*
C8/FA	1.50	1.69	2.24	8.30*

*specimens eventually disintegrated following maximum water uptake.

Table 2. Modulus, glass transition (by DMA) and fracture properties of fluoroepoxy resins[9].

Formulation	K_{Ic} ($MNm^{-3/2}$)	G_{Ic} (Jm^{-2})	E (GPa)	σ_f (MPa)	ε_f (%)	Tg (°C)
C_6/1SA	0.488	120.8	1.74	42.79	2.6	61
C_8/1SA	0.548	160.0	1.66	41.72	2.7	56
C_8/FA*	0.455	76.3	2.38	40.72	1.7	116

* cure conditions and accelerator employed different to that used for water absorption studies.

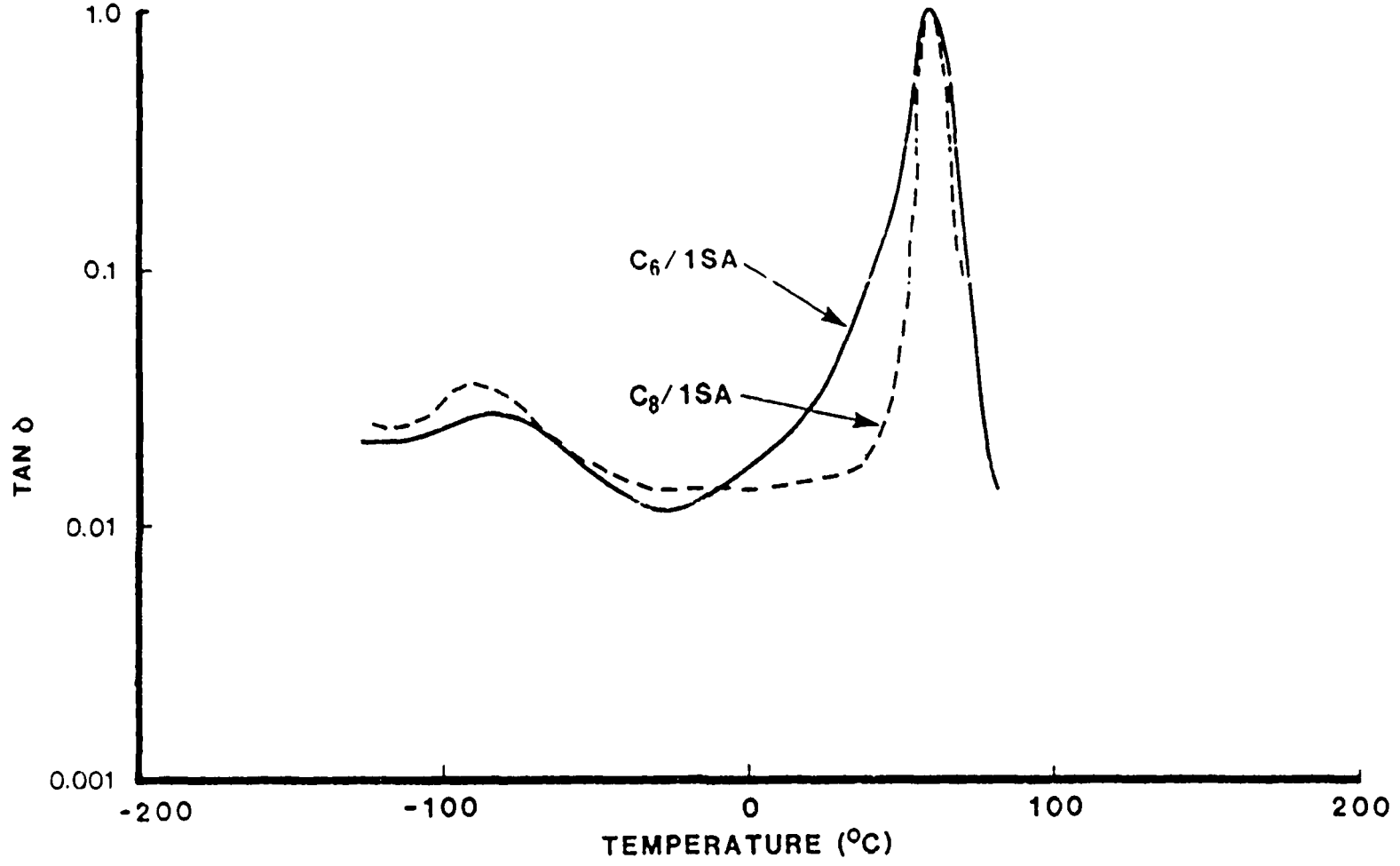

Figure 1. DMA of C8/1SA and C6/1SA neat resins[10].

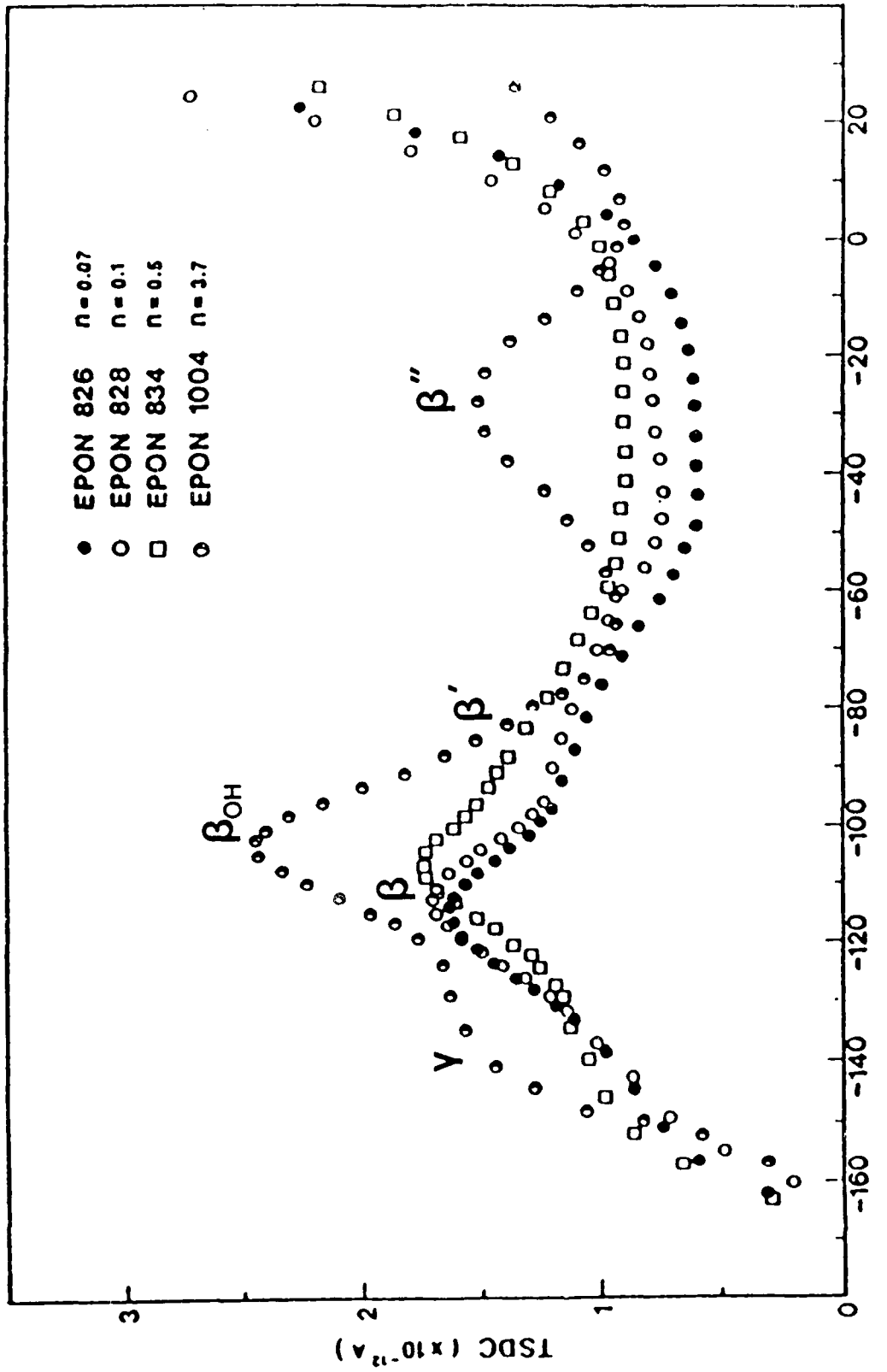

Figure 2. Low temperature TSC of DGEBA illustrating the γ, β, β_{OH}, β' and β'' type transitions.[13]

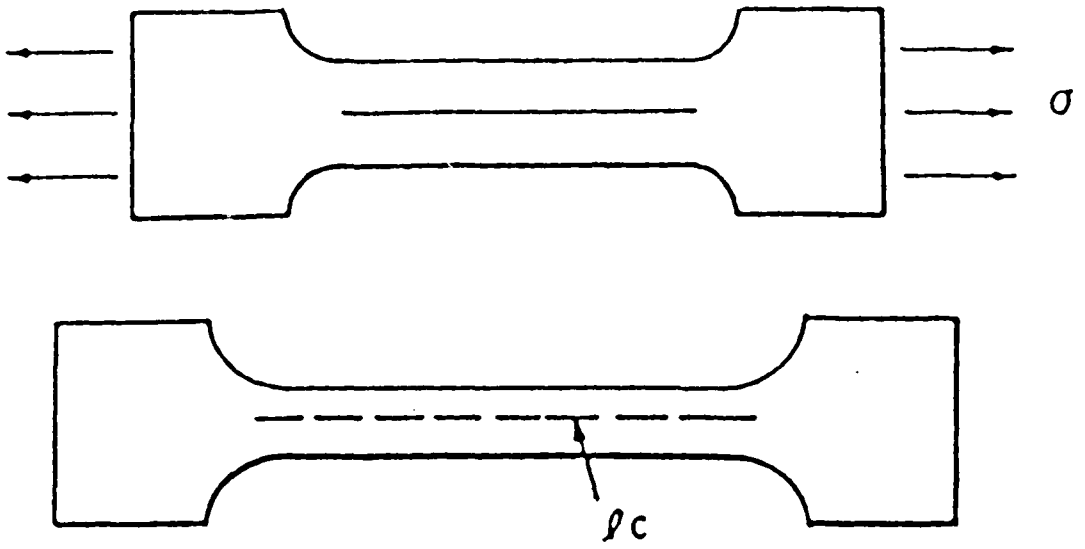

Figure 3. Single fiber tensile dogbone sample illustration.[14]

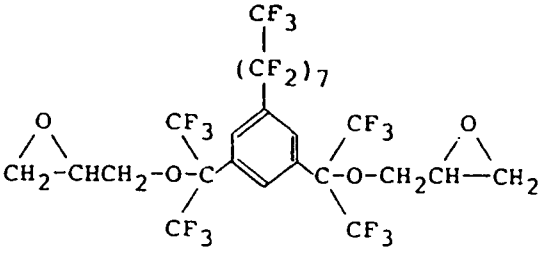

NAVY C-8 RESIN

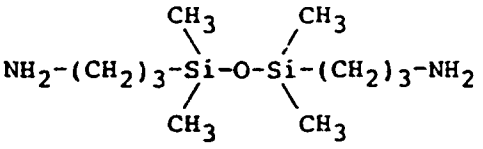

SILICONE DIAMINE CURING AGENT

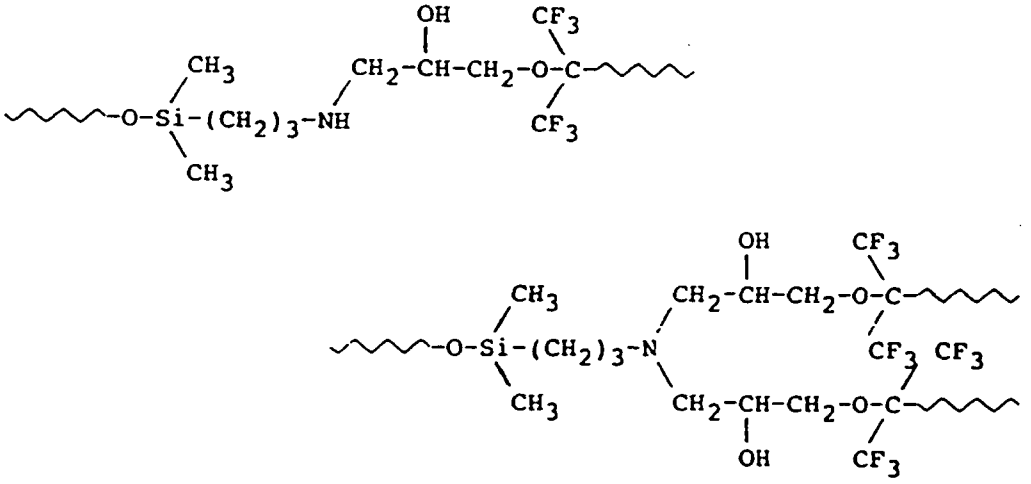

LIKELY CURING CONFIGURATIONS

Figure 4. Curing chemistry of C[8]/[1]SA resins.

2. RESIN CHARACTERIZATION

2.1 Experimental

Casting Films and Sample Molding

For thin films for TSC and DSC, two slabs of RTV 11 silicone rubber (General Electric) were molded on polished steel plates and coated with Bomb Lube Yellow mold release (Price-Driscol). Stoichiometric amounts of the C8 resin and 1SA hardener, furnished by J. Griffith, NRL, were stirred for 20 min. at a temperature of 50-60°C, the window of miscibility for the two agents. The reacting mixture was then poured onto the smooth surface of one silicone casting. The mixture was degassed under vacuum for 20 min. The second smooth molded surface was then pressed over the puddle of liquid. This assemblage was allowed to cure at room temperature for at least 16 hours. At this time, postcuring was applied as appropriate. A given specimen was not removed from its mold until its curing cycle was complete.

Where molded samples, such as dogbones or rectangular pieces were required, a female RTV 11 mold of the desired dimensions was used. The cavities were filled with the reacting mixture as above, degassed and covered with a flat silicone rubber slab. Molded samples were all cured at room

temperature for 16 hours under an N_2 atmosphere and postcured for 3 hours at 120°C.

DSC Studies of Glass Transition

DSC studies were carried out using a Perkin-Elmer DSC 4. Films were cast, and portions were cut off and crimped into standard Perkin-Elmer DSC pans. Non-postcured and fully postcured samples were run scanned for comparison. One experiment was carried out in situ, postcuring a non-postcured specimen for various lengths of time in the DSC at 160°C. Another experiment compared the transition behavior near room temperature of samples postcured for various lengths of time at 80°C.

To resolve the nature of an unidentified peak in the above experiments, the presence of various potential reactive groups in a non-postcured sample was investigated using an FTIR technique. In addition, DSC scans were run of pure 1SA hardener in both the pure state and when crystallized by the presence of CO_2.

TSC of Low Temperature Transitions

While our primary interest was in room temperature transitions, we also examined the low temperature transitions of the material. Room temperature polarization was required to allow the distinguishing of peaks from the noise at lower temperatures. A Toyoseiki TSC was used. Small (1.5 cm^2 × 0.2 mm thick) pieces of fluoroepoxy film with 20

min. of postcuring at 120°C were plated on both sides with 1 cm. diameter gold electrodes by evaporation. In order for the samples to be satisfactory for measurement it was required that the electrodes have a surface resistance of less than five ohms and that there be an infinite resistance through the sample. The sample was polarized for 30 min. at room temperature using a 10,000 V/cm field.

TSC of High Temperature Transitions

The same system described above was used to characterize the transitions of fluoroepoxy near room temperature. Electrodes were plated in the same manner. Most samples had 1 cm. electrodes, but in one case a 1 inch diameter electrode was used. Samples were postcured for 10 min. at 120°C and polarized for various times at 120°C. The total postcuring was the sum of these two time periods. All samples were polarized in a 10,000 V/cm field.

Tensile Measurements: Deflection

2.5×0.5×3/8 (length × width × thickness) inch dogbone samples with a 1.5×0.25 (l×w) inch gauge dimension were cast as described above. The aging histories of these samples were removed[c] just prior to testing. The samples were tested in tension in an Instron 1551. Initial strain measurements were made using a knife edge extensometer with a

[c]by heating to 120°C for over one-half hour.

0.5 inch gauge length. The Instron was fitted with a thermocouple controlled oven. The tensile behavior was recorded for both 28°C (room temperature) and 45°C.

Tensile Measurements: Aging

Rectangular tensile samples 2.5×0.5×1/8 inch were fully cured and allowed to age for one year. The samples were tested in tension at room temperature using a MTS 810. Here also, the strain measurement was taken with a knife blade extensometer.

Aging Effects

Portions of a fully postcured rectangular sample 2.5×0.5×1/8 inch in dimension were cut after varying periods of time. The DSC-4 was used to track the behavior of the amount of aging as a function of time elapsed.

Swelling

Portions of a fully cured rectangular specimen of the same dimensions reported above were soaked in acetone for various periods of time. The change in sample volume and sample weight were recorded.

2.2 Results and Discussion

DSC Measurements

Standard Cure

Figure 5 shows the DSC scans of a non-postcured (A) and a fully postcured fluoroepoxy (B) sample. The T_g shifts to higher temperatures, as is expected with the postcuring of a thermosetting material. The peak present at the T_g of the fully cured material is due to aging, and will be discussed later.

160°C In Situ Postcuring

The in-situ postcuring at 160°C resulted in a change in the location and form of the glass transition peak (Table 3). The lowering of T_g by 10.29 degrees and the broadening of the transition is indicative of degradation, according to Turi[11], suggesting that a postcure temperature of 160°C is too high.

80°C Postcuring

The effects of 80°C postcuring are illustrated in Figure 6. As can be seen, T_g hardly changes at all, contrary to normal behavior. There is also a peak at approximately 80°C which lowers slightly with increased postcure at 80°C. The origin of this peak was at first unknown. However, the expected residual exotherm[11] characteristic of an under cured epoxy above its T_g[d] is not evident until

after this peak. This suggested that the peak represented the freeing (melting) of some form of structure that blocked any curing at 80°C. This would explain why T_g did not advance as expected.

Still, the nature of the peak was as yet really a guess. FTIR of an unpostcured sample reflected the presence of few $-NH_2$ and -NH- groups which should be present if unreacted curing agent were present. Something seemed to be tying up the amine crosslinking agent. DSC was run on crystals of the silicone amine formed by the presence of CO_2. These crystals "melted", the CO_2 coming off, predominantly in a range from 85 to 100°C (although some portion was still melting as high as 130°C) which is consistant with the unidentified peak. This peak was not present in the CO_2 free 1SA. So it seems that when curing in the presence of CO_2, the hardener will absorb the CO_2 which will inhibit a complete cure.

TSC Measurements

Low Temperature Transitions

The low temperature TSC scan of the fluoroepoxy resin with a postcure of 20 min. is illustrated in Figure 7. Three peaks are evident. The γ peak is present as a shoulder at a temperature of -125°C. This peak is located in the same range as the γ peak seen by Pangrle, et. al. Assuming

[d]The residual exotherm is the result of postcuring reactions that begin to occur after T_g is passed.

the assignment by Pangrle, et. al. is correct, we suggest that this motion may be associated with onset of motion of the phenyl and CF_3 groups:

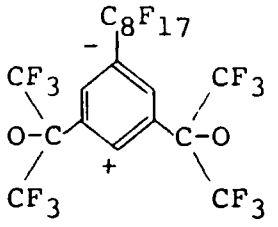

where the very electron withdrawing groups around the phenyl give it a net positive charge while the strongly electronegative fluorines in the side chain will impart a net negative charge. Note that the very small fluorine atoms may enable this portion of the chain to move relatively easily.

There is also a β peak located at -112°C. This peak is consistant with the β_{OH} peak found in the work by Pangrle, et. al., to be due to the motion of hydroxy-ether linkages:

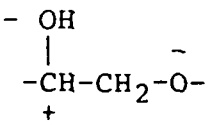

In the C8 resin, such functional groups are present, and the TSC peak indicates the onset of movement of the crosslinks to which they are attached (see figure 4).

The higher temperature β" peak (-25°C) has been assigned as an interaction with CO_2, which has been found to be associated with undercured samples when no precautions have been taken during cure. This is consistant with the

interaction of water assigned to a similar peak in DGEBA resins.

High Temperature Transitions

In Figure 8 the progress of T_g as a function of extent of postcure is readily apparent. The lowest curve, having a minimum of postcuring, shows a T_g of 35°C with a possible shoulder at 15°C due to a less densely crosslinked phase. As postcuring progresses both peaks shift to higher temperatures, the predominate T_g peak shifting to 65°C. The change in shape indicates that a significant portion of the material retains a much lower T_g, as is shown by the shoulder of the "fully" cured specimen scan at approximately 45°C, ie. there are domains representing two degrees of crosslinking.

The higher temperature peak that shifts from 60 to 75°C has been asigned as a ρ peak. Some scientists report that a ρ peak often occurs about 30° above the glass transition, the result of heterogeneous charge injection. Despite the near disappearance at the full cure, such an assignment seems most reasonable at this time. The height of this peak is known to vary considerable from sample to sample, even in supposedly identical samples.

Correlations of DSC and TSC Observations

From the above information, it has been determined that the presence of atmospheric CO_2 is a strong deterrent to

cure. The crystals formed block curing at any temperature below approximately 90°C, and even slow curing at 120°C to such an extent that more than 3 hours are required to reach a full cure. While both DSC and TSC substantiated the T_g found by Shaw, the high resolution afforded by the TSC technique showed the presence of a very broad transition starting at approximately 40°C, even for fully cured samples. This indicates that C8/1SA is indeed a low temperature material.

Mechanical Properties

Tensile Modulus and Deflection

Figure 9 shows the stress-strain behavior in tension of C8/1SA resin at 28 and 45°C. The room temperature testing showed a modulus of 194 ksi, while the 45°C experiment showed a significant drop in modulus to 46 ksi. The room temperature modulus is consistant with that measured by Shaw[10]. Thus, the material undergoes a significant drop in properties, such as modulus, at a temperature between 28 and 45°C. This is consistent with the data gathered by TSC. While the material yielded in a ductile fashion at both temperatures, it behaved much more plastically at the elevated temperature.

The room temperature sample yielded and failed at the position where the extensometer knife edge was impressed on the specimen. The higher temperature sample yielded and drew uniformly up to the maximum stroke range (2 inches) of

the Instron. Thus the failure stress and strain could not be measured for either sample. The noise in the high temperature scan is due to the weakness of the signal being generated in relation to the scale of the load cell which was available.

Tensile Modulus and Aging

Figure 10 demonstrates the change in stress-strain behavior in tension of the C8/1SA resin as a function of sample age. The 1 year old sample showed a modulus of 260 ksi, a slight improvement over the 194 ksi seen in a fresh sample. The largest effect by far however, is the radical change from ductile to brittle failure in just 1 year. Clearly, in the early days in the C8/1SA lifetime, the mechanical behavior will change from day to day.

Note also that the two moduli measured for a fresh sample and a fully aged sample bracketed the modulus reported by Shaw. Here, also, failure data was unobtainable, this time due to failure in the grips.

Physical Aging

Figure 11 shows the progress of physical aging as observed by DSC. In a fresh, fully postcured sample there is a slight change in baseline at approximately 65 °C indicative of T_g, as would be expected for a fully cured, tightly crosslinked sample. As time progresses, however, a peak develops at the T_g, increasing rapidly, until after only 77

days it reaches approximately 95% of its total equilibrium height (the peak height of a 1 yr. old sample is only slightly greater). This peak is indicative of physical aging, a natural process during which the free volume of a polymer gradually shrinks. C8/1SA undergoes rapid aging compared to epoxies. On the other hand, after 6 months, the C8/1SA resin has reached its full aging, and properties should undergo no severe change after this point. If the aged properties are those desired, the means for a stable product are just a matter of time.

Swelling

The C8/1SA resin swelled rapidly in acetone, eventually absorbing enough to cause the specimen to rupture. Radial cracks formed as differential solvent absorption through the thickness of the sample caused the rupture of bonds. The destructive failure of the sample limits the value of swelling experiments for this material, making measurements of crosslink density by swelling impossible.

2.3 Conclusions

Although the C8/1SA resin has been found to have desireable frictional, surface tension, fire resistant and above all water uptake characteristics, neat resin characterization brings many hidden difficulties to light. First, processing must occur under inert atmospheres to avoid

adsorbing CO_2 with the associated difficulties in curing. Second, the initial properties of the material will change rapidly as the fluoroepoxy undergoes physical aging. The material is of moderate strength, but has a low T_g and a heat deflection temperature (indicated by the drop in properties between 28 and 45°C) too near to room temperature for practical applications. The low temperature transitions, also seen to be mechanically active in Shaw's DMA work[10] indicate that this material should be at least as tough as a regular epoxy. However, C8/1SA would be of limited use as a purely structural material.

Table 3. 160°C Postcuring

Time of Postcure	T_g Onset	T_g Midpoint
0 min	27.45	31.57
5 min	17.16	28.15

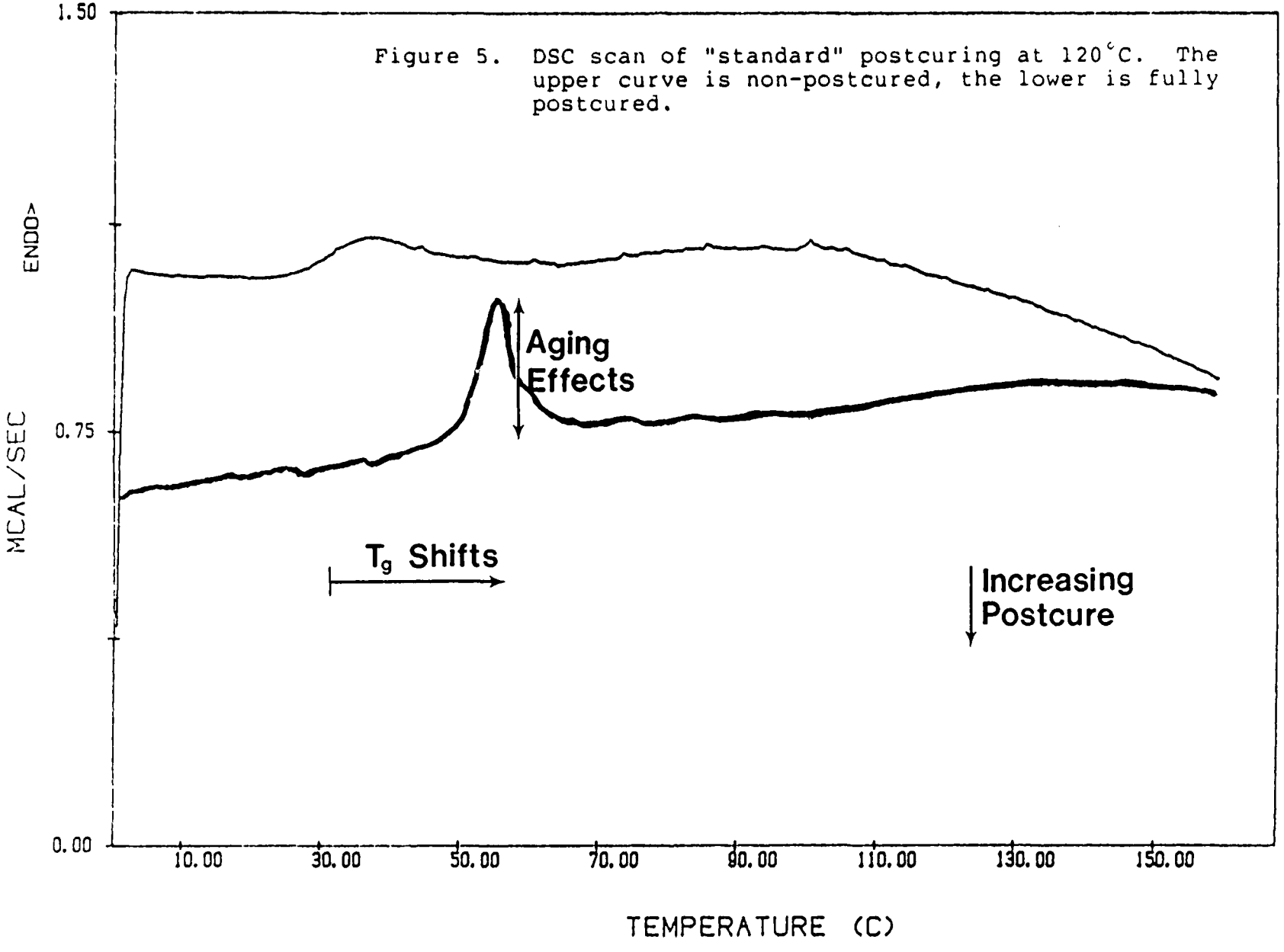

Figure 5. DSC scan of "standard" postcuring at 120°C. The upper curve is non-postcured, the lower is fully postcured.

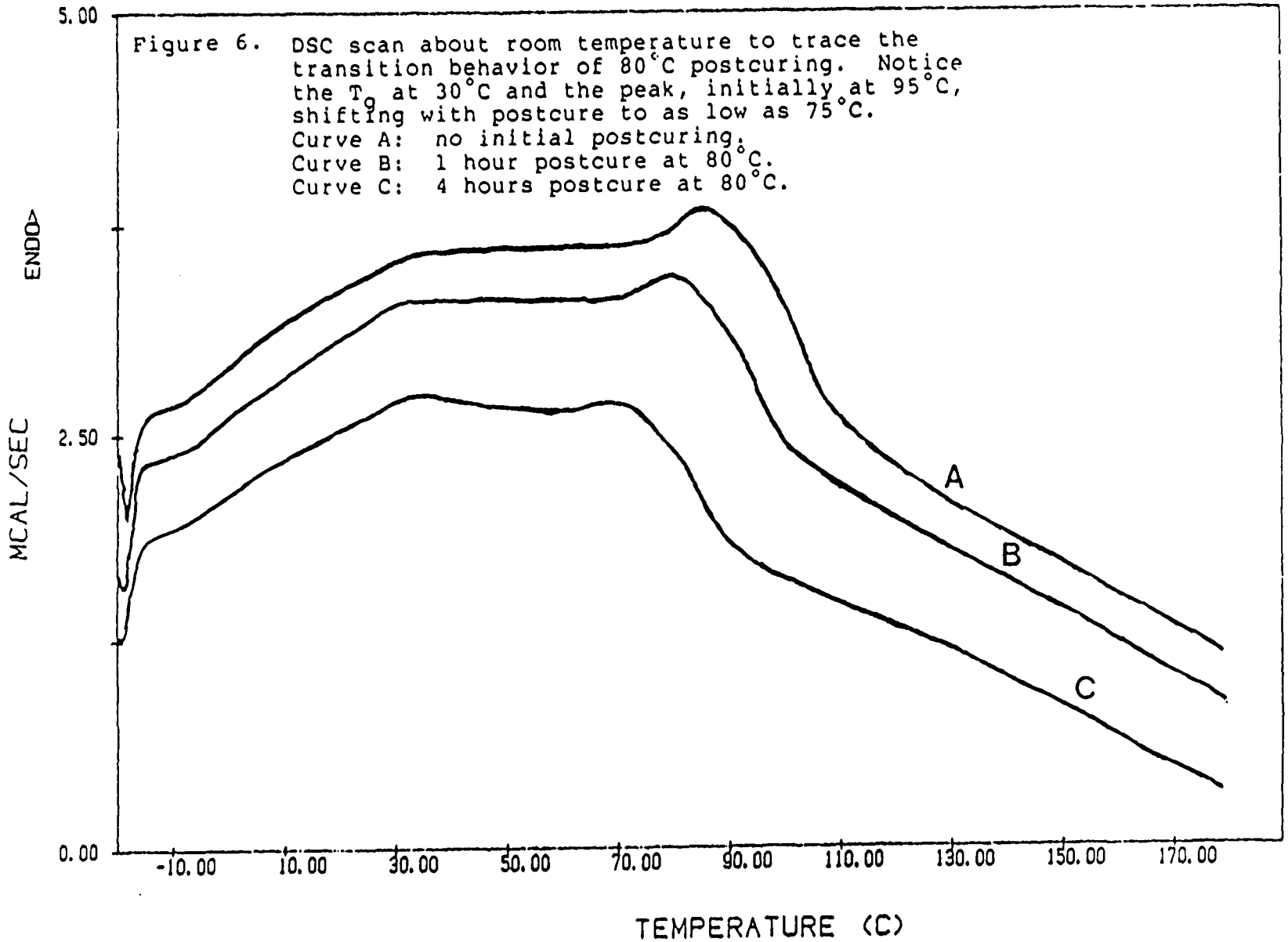

Figure 6. DSC scan about room temperature to trace the transition behavior of 80°C postcuring. Notice the T_g at 30°C and the peak, initially at 95°C, shifting with postcure to as low as 75°C.
Curve A: no initial postcuring.
Curve B: 1 hour postcure at 80°C.
Curve C: 4 hours postcure at 80°C.

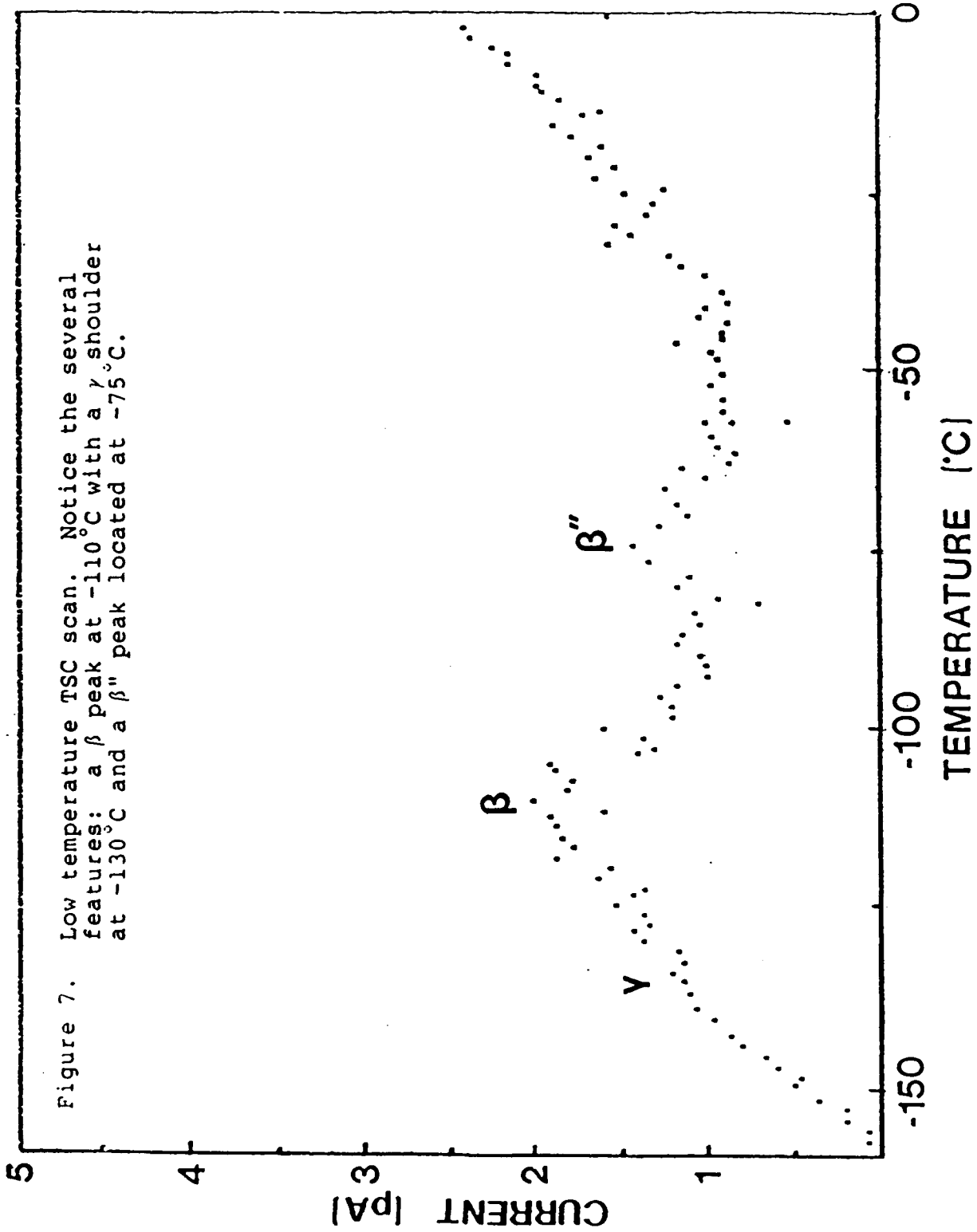

Figure 7. Low temperature TSC scan. Notice the several features: a β peak at -110°C with a γ shoulder at -130°C and a β" peak located at -75°C.

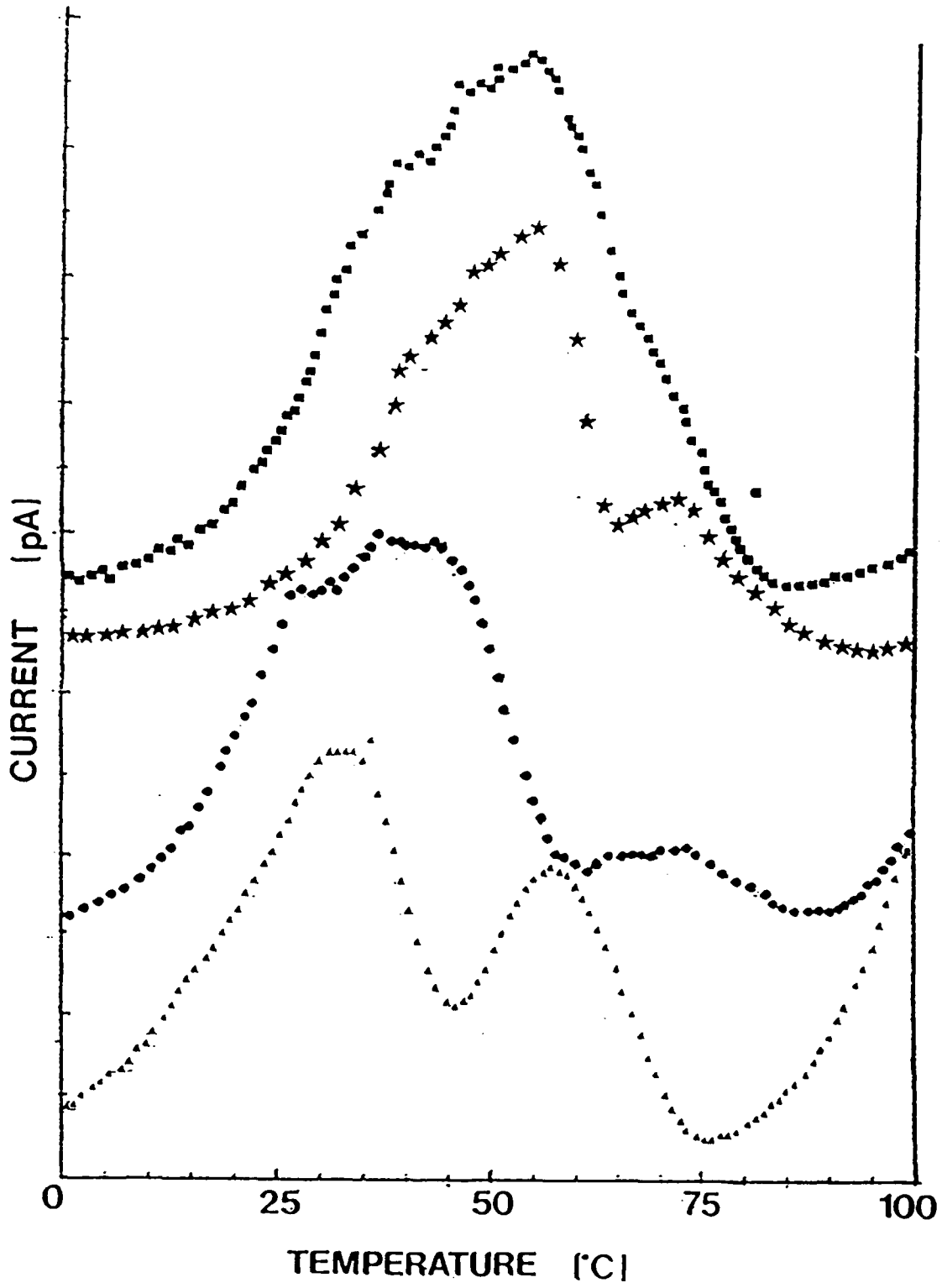

Figure 8. TSC scan about room temperature to trace the transition behavior as a function of 120°C post-curing. (▲) 20 min., (●) 1 hour, (★) 3 hours, (■) 3.25 hours.

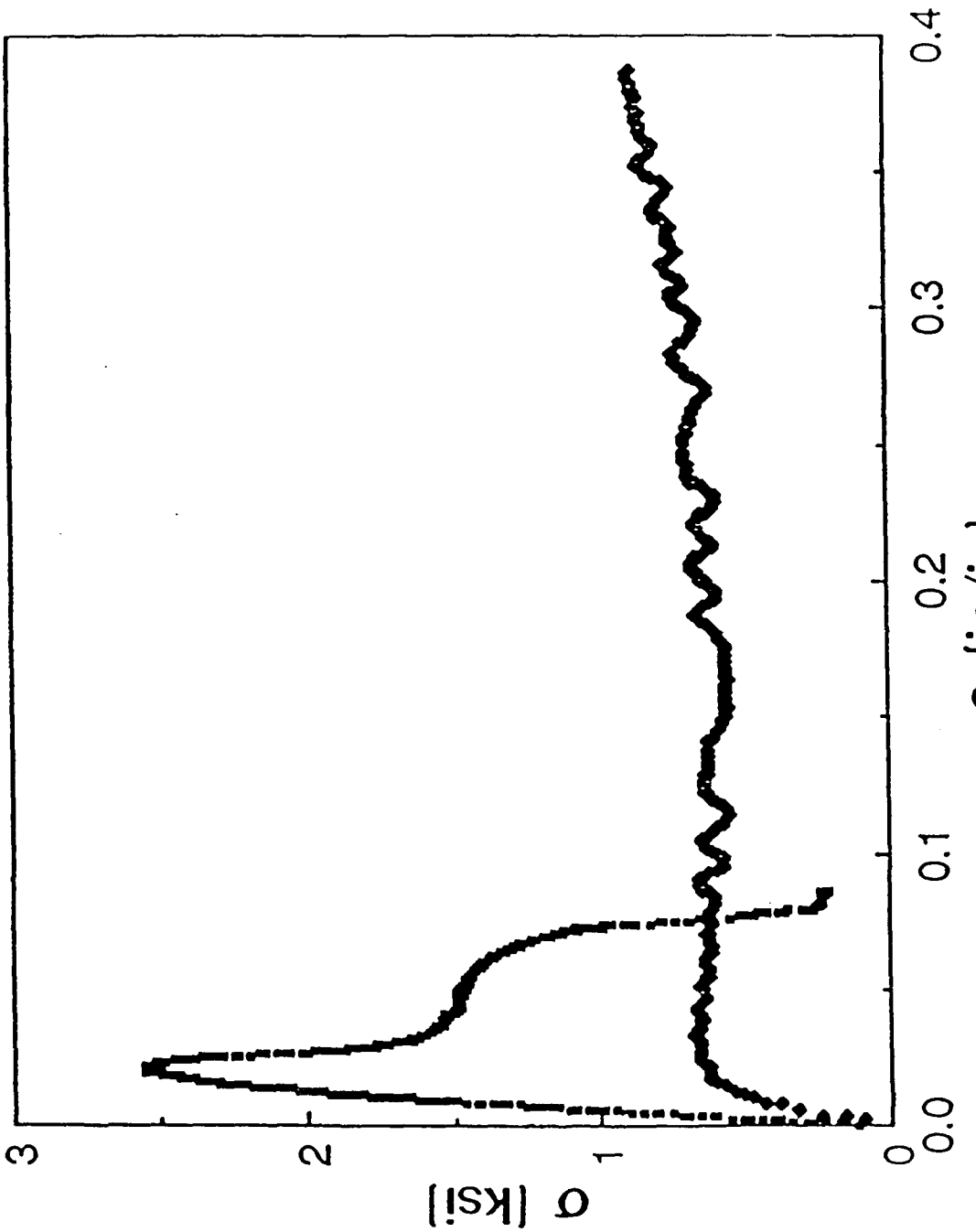

Figure 9. Stress-strain behavior of C8/1SA at (•) room temperature and (◆) 45°C.

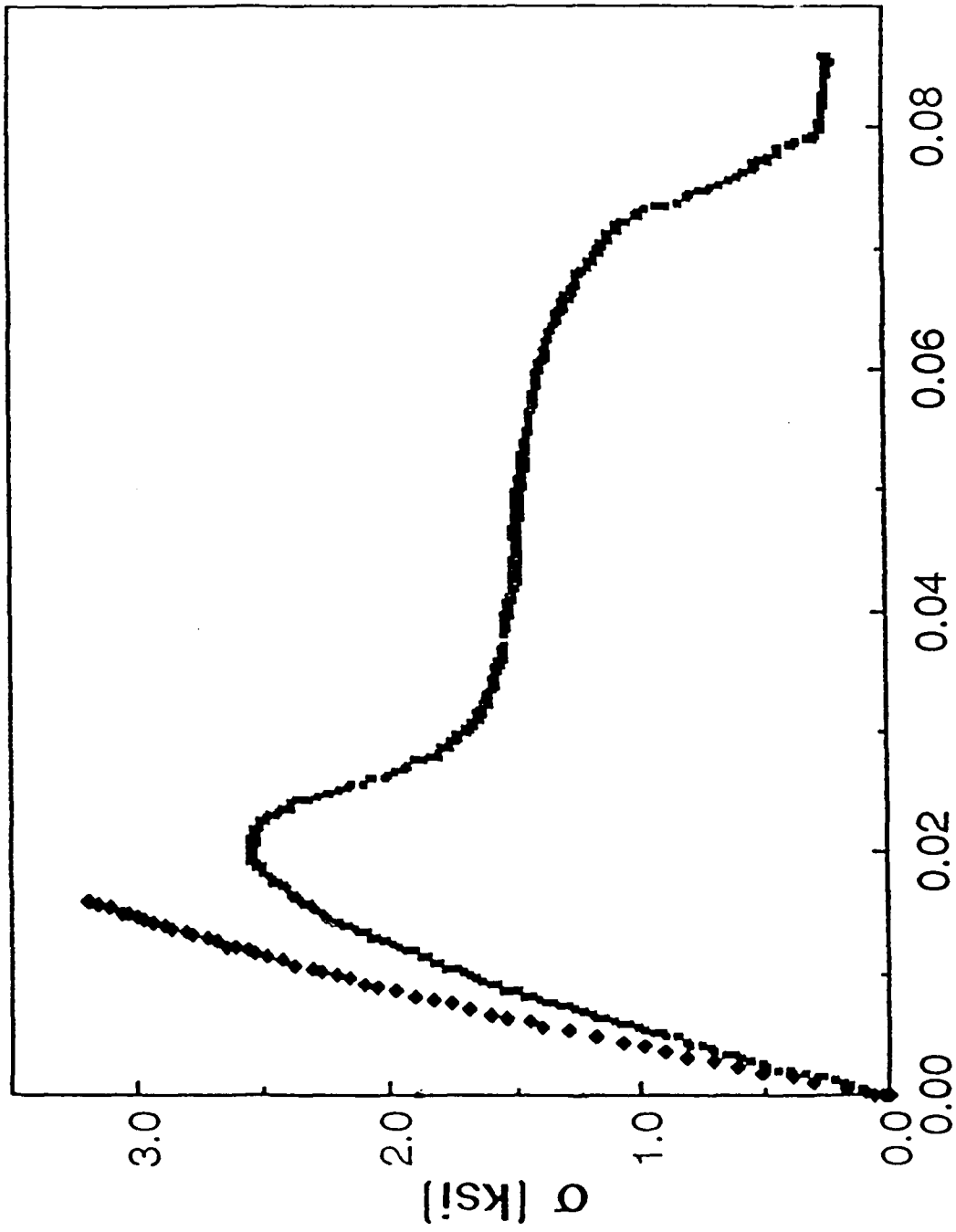

Figure 10. Stress-strain behavior of C8/1SA both (•) fresh and (◆) aged for 1 year.

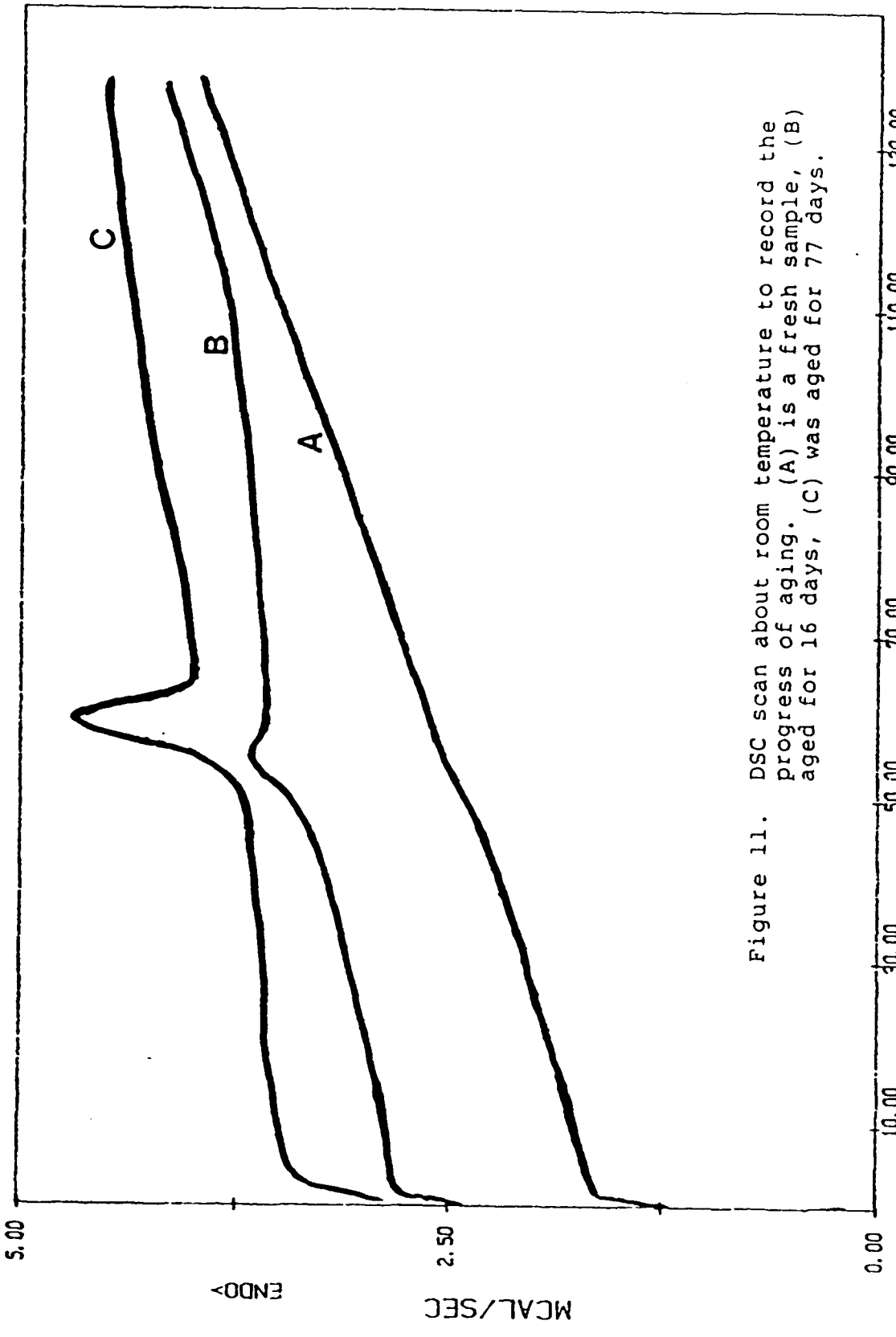

Figure 11. DSC scan about room temperature to record the progress of aging. (A) is a fresh sample, (B) aged for 16 days, (C) was aged for 77 days.

3. BLEND WITH EPON 828

3.1 Experimental

Material Preparation

10% C8/1SA by weight was blended with Epon 828. This mixture of resins was mixed with a stoichiometric amount of 1SA hardener. The resin was then stirred for 20 min. at a temperature of 50 to 52°C, the lower end of the hardener-C8 miscibility window, which was somewhat higher than the Epon 828 miscibility window, Epon becoming miscible at as low as 40°C. The lower temperature was selected to prolong pot life. The reacting mixture, a nacreous mixture due to the fundamental immiscibility of C8 and Epon 828, was decanted into silicone molds in order to cast free surfaces, films and dogbone samples of the same sort used in characterizing the neat C8/1SA resin. The sample was outgassed under vacuum for 20 min. at room temperature. Cure schedule varied from sample to sample.

The cure was accomplished in two ways. The slow route involved curing the outgassed sample under N_2 for 16 hours at room temperature followed by a 3 hour, 120°C postcure. The fast route entailed a 60°C cure for 1 hour, followed by 15 hours at room temperature during which, presumeably, no further reaction occurred, and 3 hours of postcure at 120°C, all conducted in an inert atmosphere.

For electron microscopy, the blend was in many cases etched to enhance the morphology, as fluorinated materials are very susceptible to ionization. A Lepel high frequency generator was used to generate a current in a cylindrical coil (Figure 12). This current generated a field in which gas (air) molecules were ionized. These ionized molecules bombarded the surface of the sample, which was maintained on a liquid N_2 cooled cold stage.

Blend Morphology

A bulk sample and a dogbone sample 2.5×0.5×1/8 inch with 1.5×0.25 inch gauge dimensions were fast cured. The bulk sample was cleaved at room temperature with a razor, etched for 1 hour and replicated[e]. The etched surface was also then coated with Au-Pd. An aged dogbone sample was fractured in flexure at room temperature. The fracture surface was shadowed with Pt-C and carbon coated. All three surfaces were examined using a Hitachi S570 SEM at 15 kV accelerating voltage, a 13 mm working distance, aperture setting 2 and both condensers set at 5.

Surface Chemistry

a Perkin Elmer Φ 5400 XPS was used to investigate the surface properties of the blend. A free surface, molded

[e]the etched surface was shadowed with Pt-C, then coated with Carbon. This thin layer was stripped with polyacrylic acid (PAA) and mounted with no further treatment.

bottom surface (against the silicone mold), and fast and slow cured "free"[f] surfaces were examined. Spectra were taken at 15° and 75° to the surface to enhance the surface and the bulk chemistry, respectively (Figure 13). The beam always penetrates 60 A, but when the sample is tilted relative to the beam the true depth is modified. Scans of neat C8/1SA and Epon 828/1SA resin were run for comparison.

Specimen Welding

Slow cured dogbone specimen of the usual dimensions were placed with the bottom surfaces in contact before the postcure was applied. Contact pressure was applied in a hot press, which was used to apply the 3 hour, 120°C postcure. The dogbones were fractured in flexure, polished, ion etched for 20 min. in an air plasma and coated for inspection in the SEM.

Tensile Properties

Using an Instron 1331, dogbone samples 2.5×0.5×1/8 inch with 1.5×0.25 gauge dimensions were deaged[g] and tested in tension. Epon 828/1SA samples cured and treated the same way were also run for comparison.

[f]A free surface is molded in such a way as to limit contamination with silicone release agent. A "free" surface is the open upper surface of a molded piece.
[g]heated at 120°C for over 1/2 hour to remove aging history.

3.2 Results and Discussion

Fractured and Etched Surfaces

The etched surface (Figure 14) shows predominantly 10-20 micron diameter spherical domains where fluoroepoxy has etched out of the Epon matrix. That these are holes is confirmed by the protrusions of similar dimension on the replica surface (Figure 15). The spherical domains are the logical consequence of the immiscibility of the C8 and Epon 828 components. These domains should be bound to the matrix by the common curing agent. Because of their ductility, at least before aging, they should serve as toughening agents by arresting cracks.

However, since the domains are immiscible in the matrix, the crosslinking agent joining the materials will perforce be located in a nearly monomolecular layer at the interface. The $Si-CH_2$ bonds are weak relative to any of the other types of bond in the materials, which might lead to a relatively low energy path of fracture around the domains. This may also serve to toughen the ordinarily brittle Epon in much the same way as fibers toughen ceramic matrices.

In Figure 16, the fracture surface is seen. There seem to be two types of domain, corresponding to spheres and holes, where spheres have pulled away. This micrograph indicates that adhesion is relatively weak at the interfaces as the fracture proceeds around the domains to the exclusion

of any other behavior. This may be due to the weakness of the curing agent or to the specimen age of two weeks.

Surface Chemistry

Figure 17 shows the XPS scan of the neat fluoroepoxy resin, oriented at both 15° and 75°. As can be seen in Table 4, there is an indication that there is a somewhat greater amount of fluorine functionality at the surface. This could be due to preferential alignment of the long fluorinated side chain at the surface of the specimen. However, the difference is not large and shall therefore be assumed for now to be due to experimental error.

Figure 18 shows the scan of the free surface of the blend. The insets show that N functionality is present to the same extent as was found in the neat resin. As the chemical composition of the surface layer was found to be nearly identical to neat resin, this indicates that the surface layer and probably the subsurface domains contain curing agent. As the Epon phase cured, it also must contain adequate curing agent. This layed to rest the fear that one or another of the resins was thermodynamically preferrable for absorbtion of the curing agent.

Referring again to Table 4, it is noted that the free surface is covered by a layer of fluoroepoxy at least 60 A thick. On the other hand, the scan of the bottom (silicone molded) surface (Figure 19) shows a much reduced fluorine content. (The presence of a large silicon content indicates

heavy contamination by the silicone mold release agent on this surface. The 75° orientations are the most reasonable selection for a consistant comparison between different samples of differing surface contaminant levels.) This indicates that the fluoroepoxy separates preferentially to the upper surface of the blend.

The slow and fast cured "free" surfaces of the blends (Figures 20 and 21, respectively) show no significant differences. Both still show that there is a layer of fluoroepoxy over 60 A thick at the surface; the rapid cure did not cause a thinning in the surface layer that was detectable by XPS.

The samples of Epon 828 were contaminated by silicone release agents. No fluorine was noticed, indicating that none of the propellents used in the mold release were retained. No measure of the percent elemental compositions were made due to the contamination.

The noise present in all scans was due to low collection times, forced by the extreme outgassing of the fluorinated materials. The energy of formation for $CF_2\cdot$, $CF_3\cdot$ and related ions is very low and occurs under the x-ray beam. The time under the beam was therefore minimized to avoid sample damage with the concurrent change in surface chemistry, this change being similar to that occurring in ion etching of the material.

Weld Characterization

Figure 22 shows the interface region of two welded plys of fluoroepoxy. One can see two types of region. The bulk region contains the characteristic 10-20 micron diameter domains which have been elongated in compression by the contact pressure applied during welding. In the interface region there appears to be a lack of C8 domains. This indicates that the lower molded (vs. "free") surface is fluoroepoxy poor. This substantiates the findings using XPS. The width of the C8 poor region (24 μm: a depth of 12 μm due to each surface) suggests that the motive force for the separation to the upper surface is due to gravitational forces rather than interfacial energies[h]. This was unexpected. In the resin form C8 is denser than Epon 828; we have no explanation at present.

The micrograph shows no separation between the materials and no obvious weld line. This indicates a "B" stage material with good welding characteristics.

Tensile Properties

The modulus of the blend was 290 ksi, comparable to that of Epon 828/1SA, with a value of 347 ksi. Epon 828 cured fully with a diamine hardener yields a material with a modulus of 477 ksi, a failure stress of 10 ksi and an ultimate elongation of 0.024 in/in[16]. The ultimate failure

[h]surface forces being measured in nano-, not micro-meters.

stress of the Epon 828/1SA was 6.6 ksi while the elongation was 0.054 in/in[16]. This indicates that either the Epon 828/1SA is a weaker material or that it is not fully cured. The slightly ductile yielding behavior reflected in the stress-strain curve (Figure 23, A) indicates that both effects are probably present. Nevertheless, behavior in the region covered seems to be dominated by the Epon matrix (Figure 23, curve B) rather than the fluoroepoxy resin (Figure 6)[i], as was desired. The blend fractured at a void, so the fracture behavior has yet to be determined.

3.3 Conclusions

A blend of 10% fluorinated epoxy, such as C8, with Epon 828 or other standard epoxies,cured with a mutually miscible hardener shows promise of being a useful structural material. Using the Epon 828/C8/1SA system as a model, the mechanical properties seem to be in line with the stronger, more mechanically useful Epon component. XPS indicates that the fluoroepoxy is found preferentially at the upper surfaces of the material, potentially yielding a process controlled method for coating plys for laminates. Welding experiments have shown that the material can form a B stage material which can be laminated easily.

[i]recall here that the neat C8/1SA modulus was 194 ksi.

Fracture appears to occur along weak domain interfaces. Also, most experiments were conducted for freshened samples; the effects of aging might change the mechanical behavior significantly. This is the more significant problem. As the blend ages, the ductile regions will become brittle and lessen the toughening abilities of the domains. Resin modifications to overcome this problem would be of value.

Work is currently under way by Griffith[17] to develop fluorinated resins with a lower T_g which would have even more ductility than the C8 resin used, and which would limit the effects of aging. These highly ductile domains would serve as a rubber toughener. In fact, the domains of 10-20 microns seem tailor made for this application. Work is also under way to develop a material which is miscible with the "standard" resin phase at elevated temperatures but immiscible at lower temperatures, allowing thermodynamic control of domain size as the resin mixture is cooled as well as mechanical control by stirring.

Table 4. Peak data for XPS curves.

Sample	Angle	Element	Peak Area (Counts)	Corrected Peak Area*	Ratio to Carbon	Relative % Comp.
Neat Resin	15°	F 1s	10879	10879	0.465	26
		O 1s	2375	3770	0.161	9
		C 1s	4792	23376	1.000	56
		Si 2p	628	3694	0.158	9
	75°	F 1s	10865	10865	0.387	23
		O 1s	3079	4887	0.174	10
		C 1s	5753	28063	1.000	60
		Si 2p	543	3194	0.114	7
Blend Free Surface	15°	F 1s	15434	15434	0.478	27
		O 1s	3080	4889	0.152	9
		C 1s	6616	32273	1.000	57
		Si 2p	653	3841	0.119	7
	75°	F 1s	11475	11475	0.424	26
		O 1s	2374	3768	0.139	8
		C 1s	5551	27078	1.000	60
		Si 2p	448	2635	0.481	6
Silicone Molded Blend Surface	15°	F 1s	2217	2217	0.274	13
		O 1s	1676	2660	0.328	16
		C 1s	1661	8102	1.000	48
		Si 2p	663	3900	0.481	23
	75°	F 1s	2153	2153	0.090	6
		O 1s	4567	7249	0.303	16
		C 1s	4898	23893	1.000	54
		Si 2p	1826	10741	0.450	24

Table 4. Peak data for XPS curves (Continued).

Sample	Angle	Element	Peak Area (Counts)	Corrected Peak Area	Ratio to Carbon	Relative % Comp.
Slow Cured "Free" Surface	15°	F 1s	11683	11683	0.503	28
		O 1s	2190	3476	0.150	9
		C 1s	4762	23229	1.000	56
		Si 2p	514	3024	0.130	7
	75°	F 1s	11340	11340	0.348	22
		O 1s	2876	4565	0.140	9
		C 1s	6675	32561	1.000	63
		Si 2p	504	2965	0.091	6
Fast Cured "Free" Surface	15°	F 1s	3337	3337	0.344	22
		O 1s	905	1436	0.148	9
		C 1s	1991	9712	1.000	63
		Si 2p	172	1012	0.104	6
	75°	F 1s	9602	10879	0.360	22
		O 1s	2691	4271	0.141	9
		C 1s	6198	30234	1.000	63
		Si 2p	487	2865	0.095	6

*Sensitivity Factors

Element	Sensitivity
F 1s	1.000
O 1s	0.630
C 1s	0.205
Si 2p	0.170

Used to calculate corrected peak area.(18)

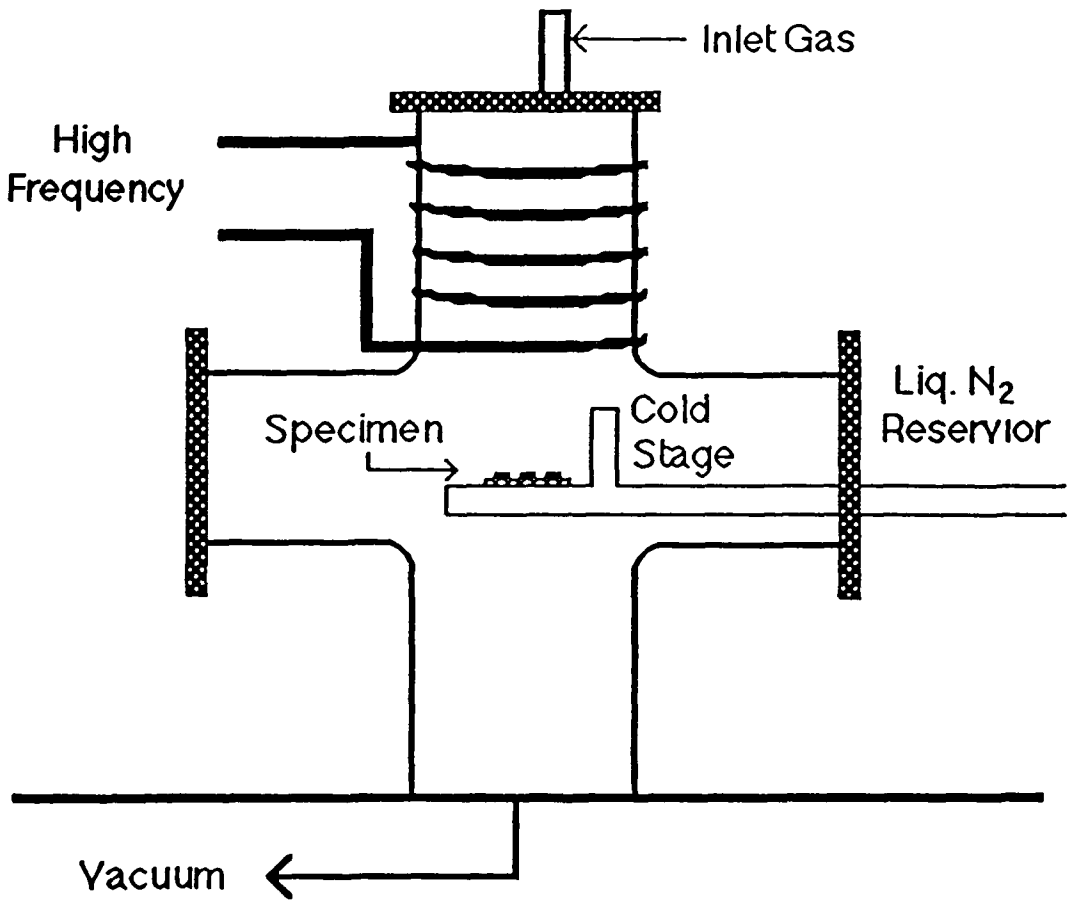

Figure 12. Ion etching aparatus.

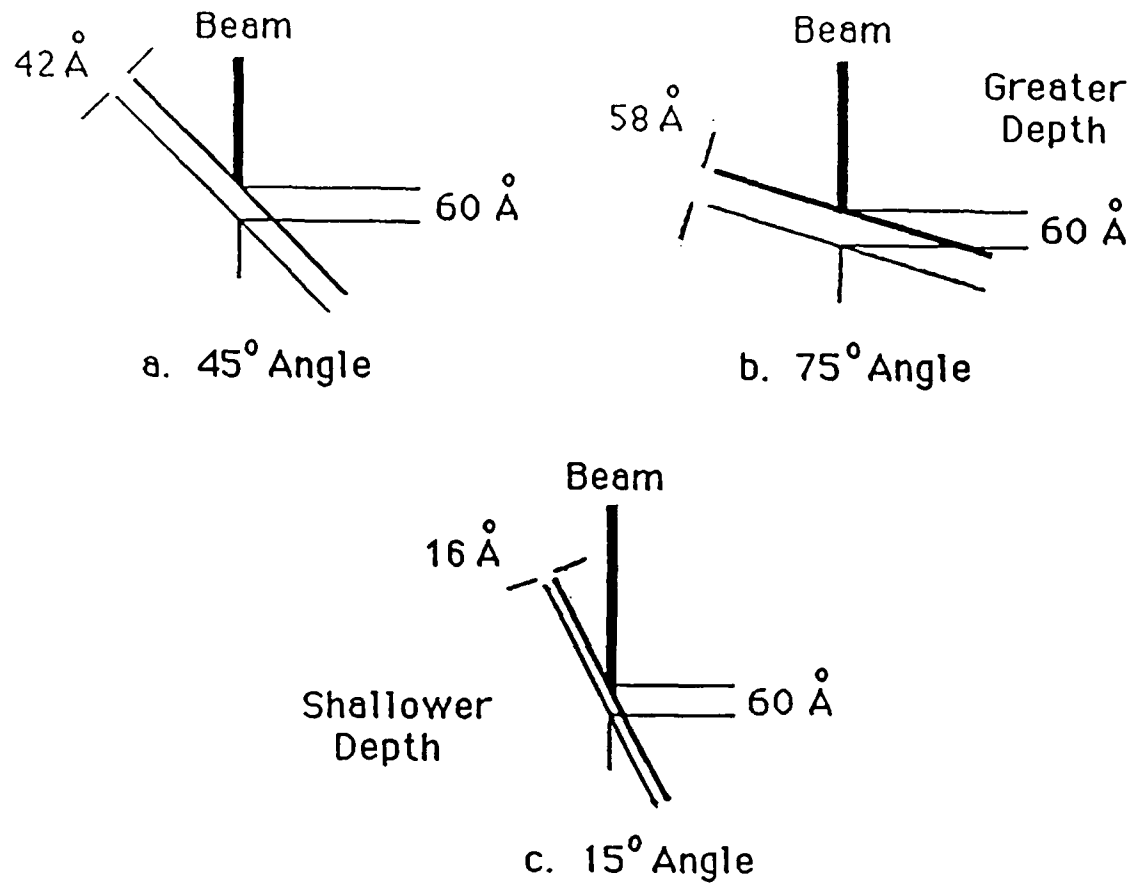

Figure 13. Effects of surface orientation on XPS information. Note that for the shallower angle more information is surface biased. For the steeper angle the bulk is emphasized.

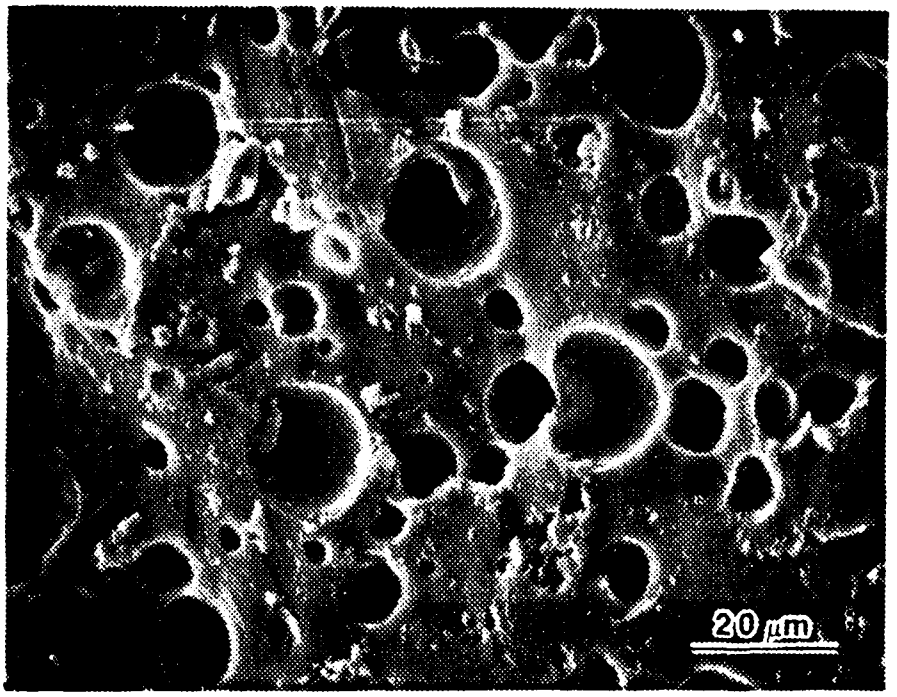

Figure 14. SEM micrograph of cut, etched surface of 10% by weight blend of C8 and Epon 828 cured with 1SA hardener. Note the spherical holes 10-20 microns in diameter where the fluorepoxy domains have been etched away.

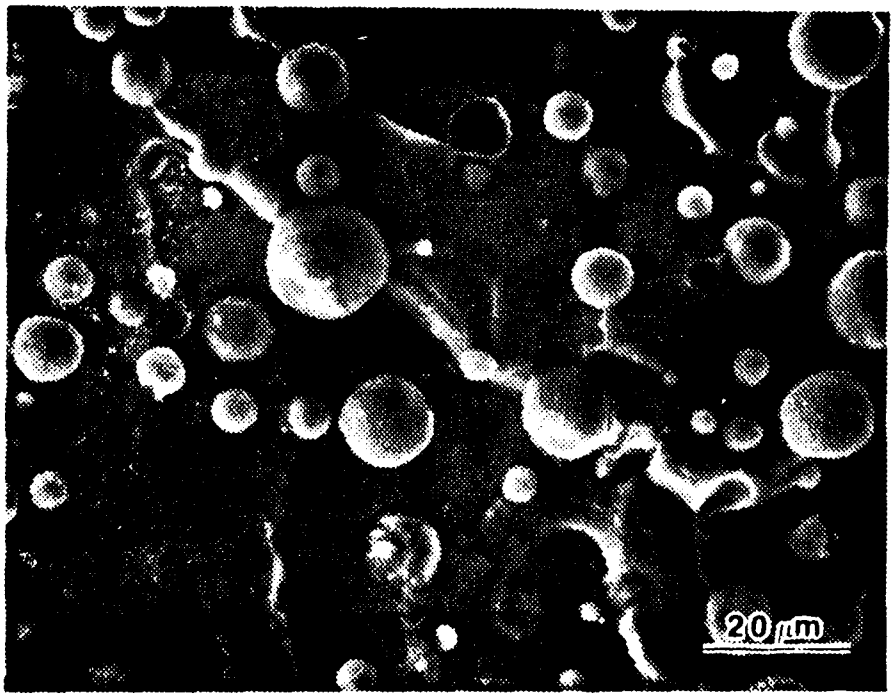

Figure 15. SEM micrograph of a Pt-C shadowed replica of the sample in Figure 14. The protrusions correspond to holes in the original sample.

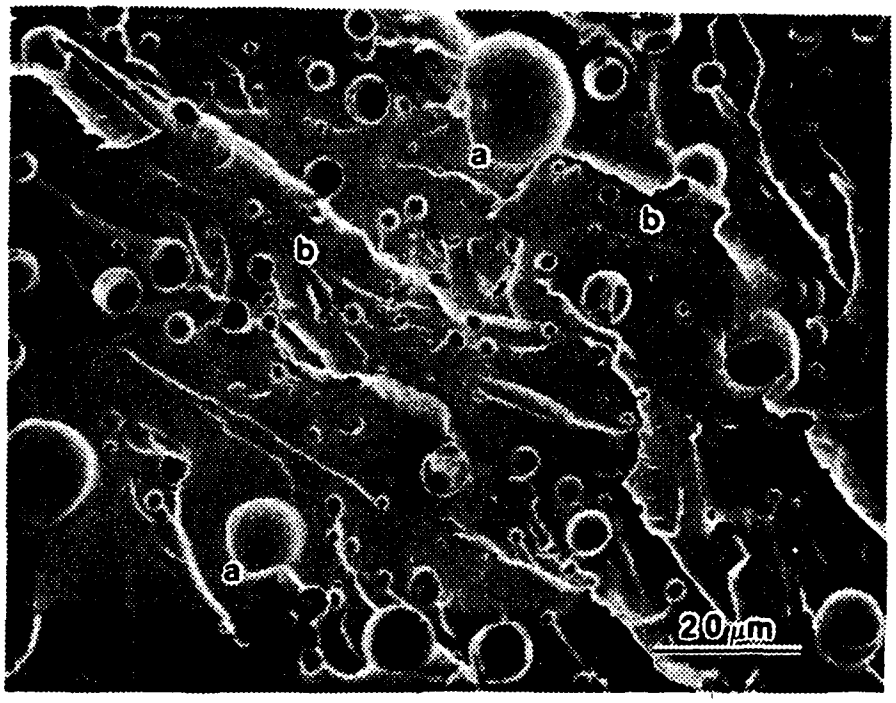

Figure 16. SEM of the flexure fracture surface of the blended material. Note (a) the protruding spheres and (b) the holes where spheres have pulled away, both indicative of a weak interface.

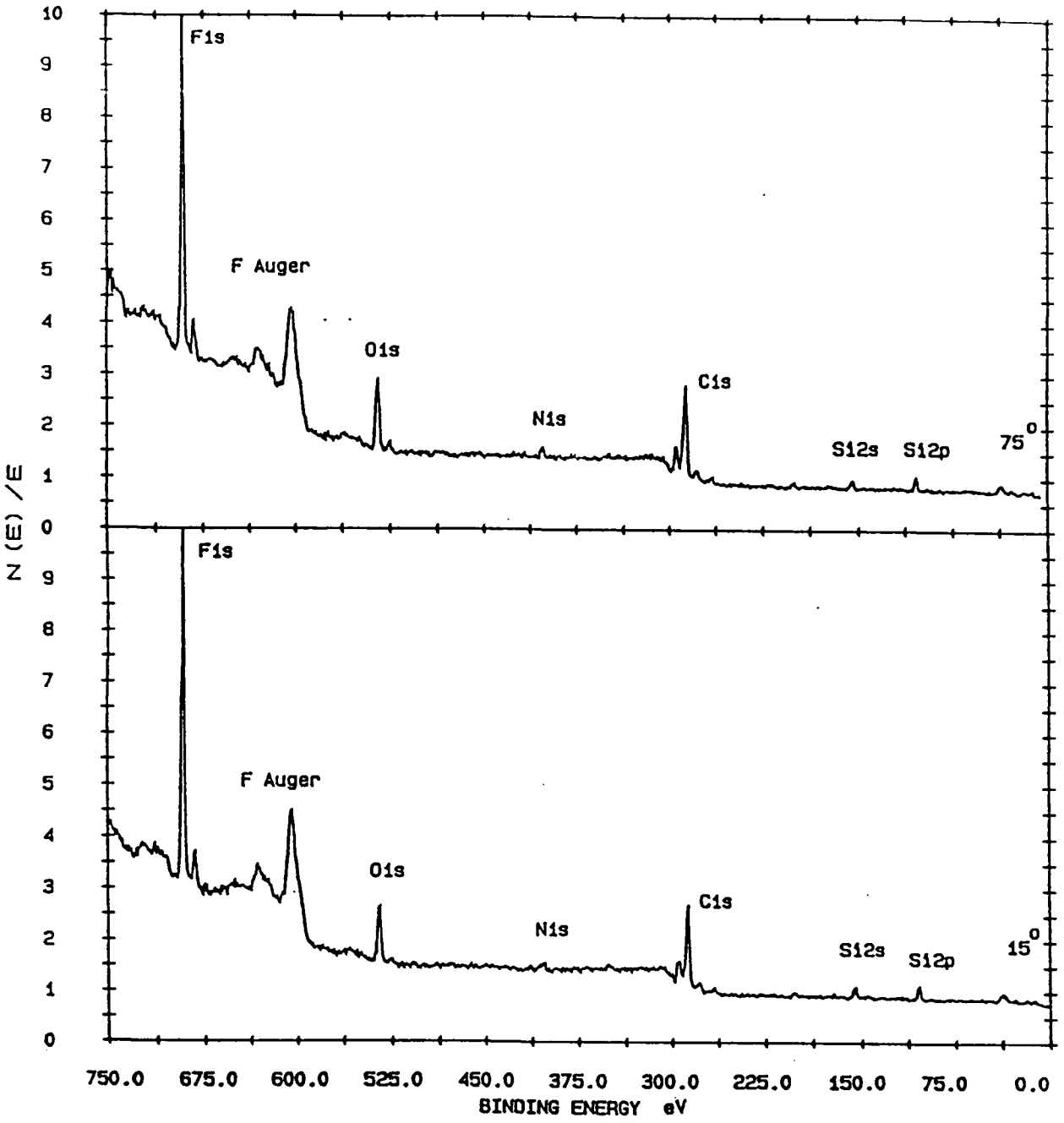

Figure 17. XPS of neat C8/1SA resin at 15° and 75°.

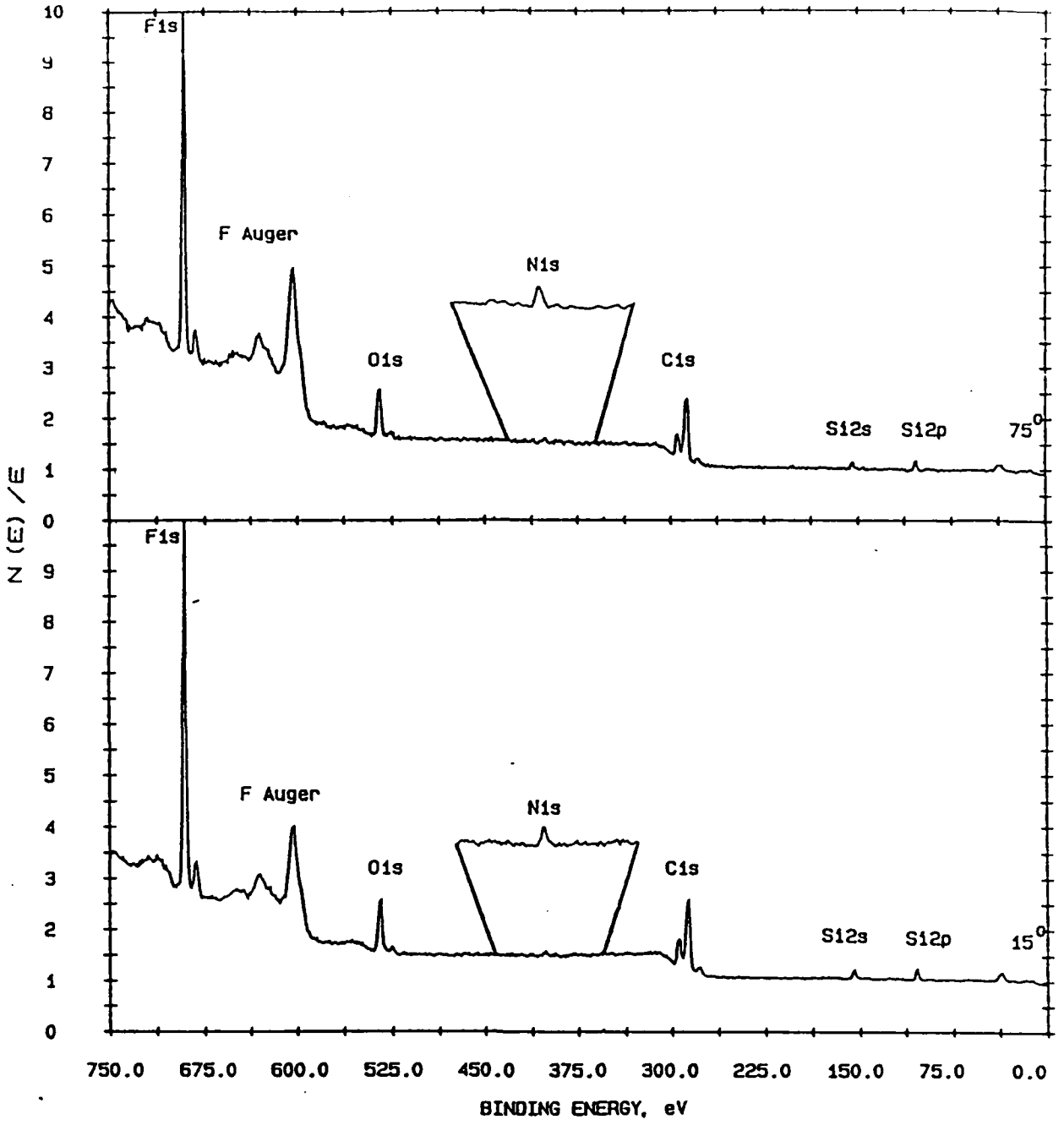

Figure 18. XPS of blend free surface at 15˚ and 75˚ with inset blow-ups of N1s peak.

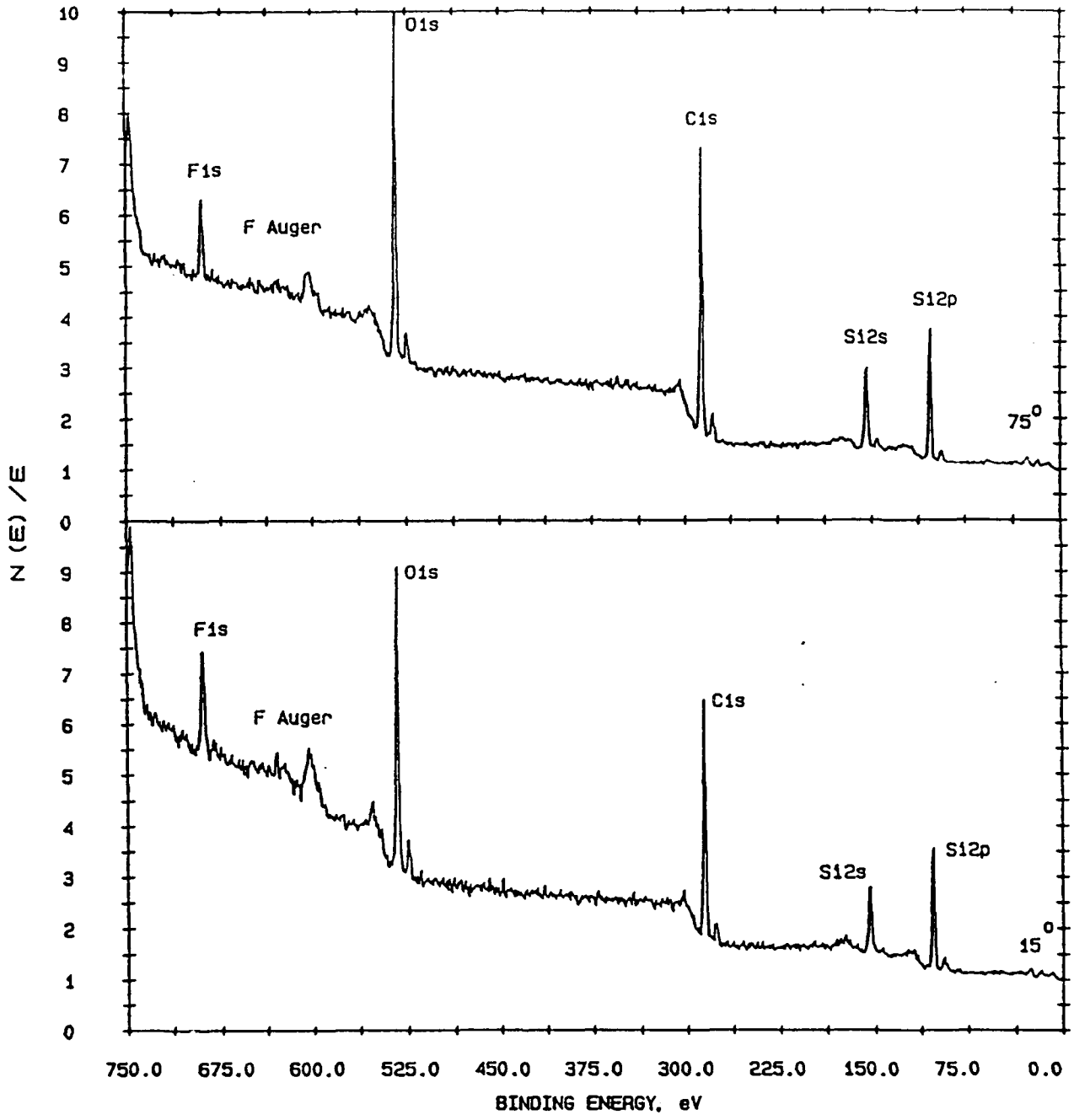

Figure 19. XPS of blend bottom (molded) surface at 15° and 75°.

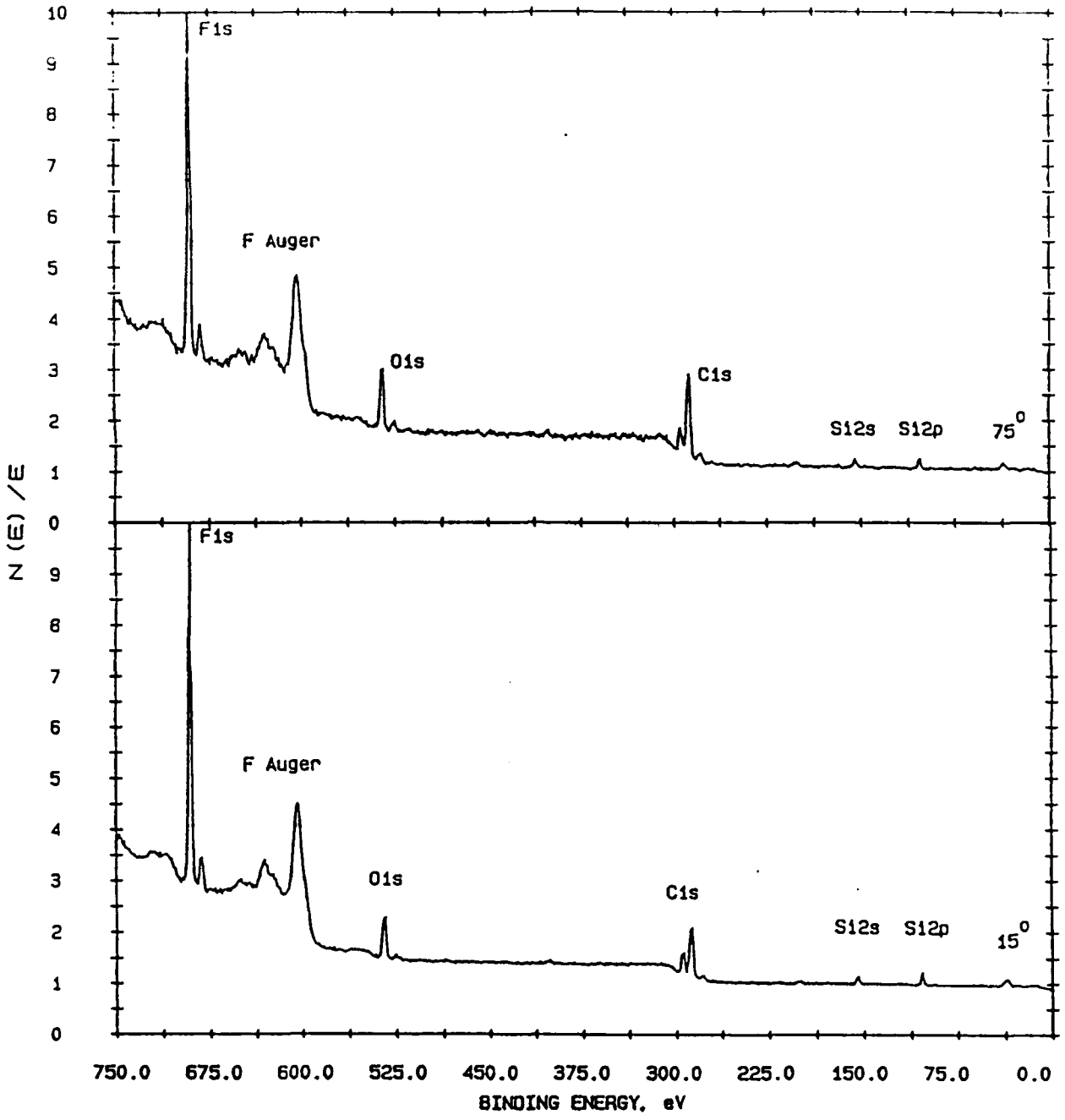

Figure 20. XPS of slow cured "free" blend surface at 15° and 75°.

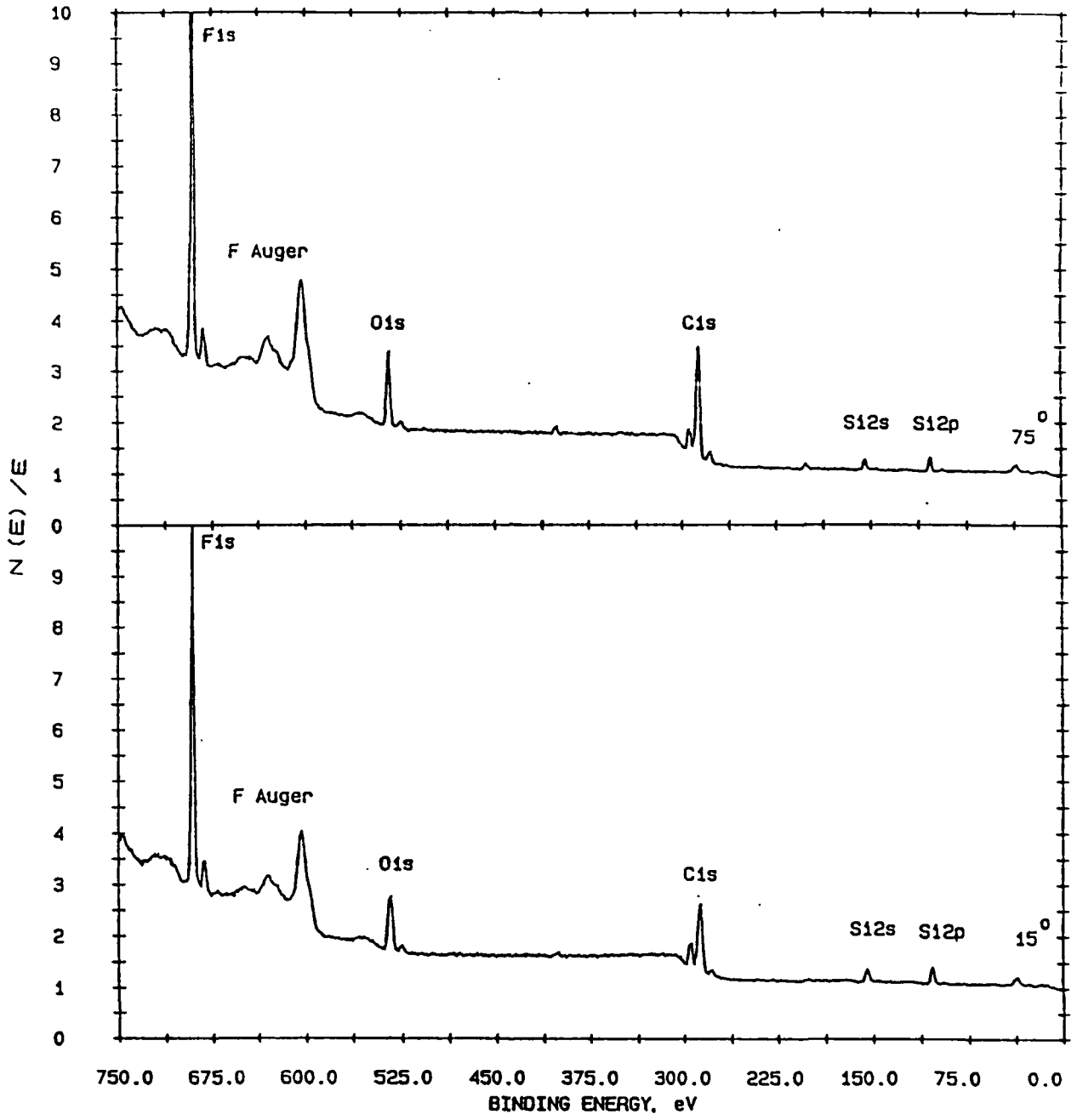

Figure 21. XPS of fast cured "free" blend surface at 15° and 75°.

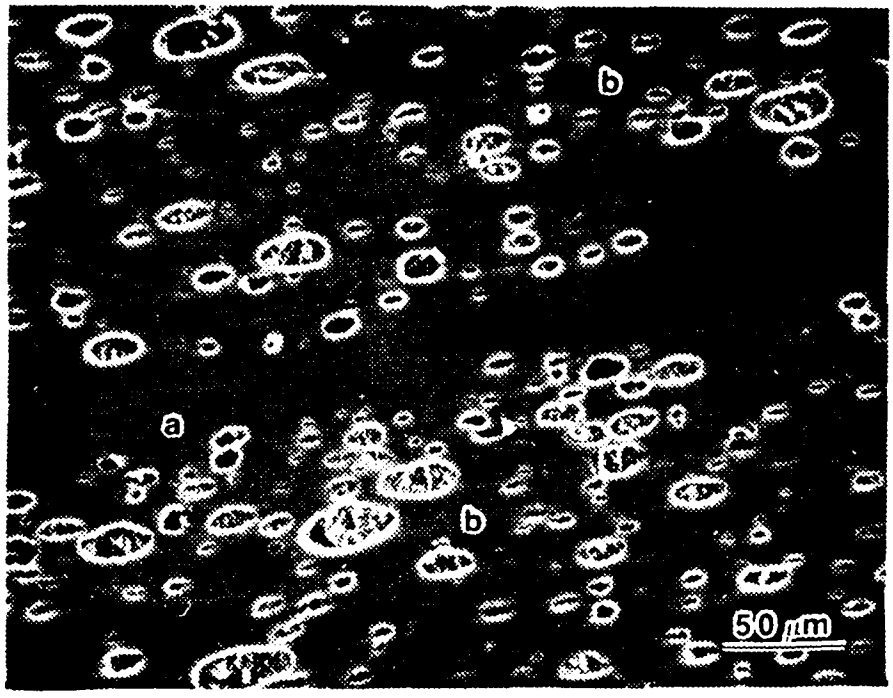

Figure 22. SEM micrograph of welded blend, surface fractured, polished and etched. Note the C8 poor region in the weld area (a) and the pressure elongated domains where fluoroepoxy has been etched away (b).

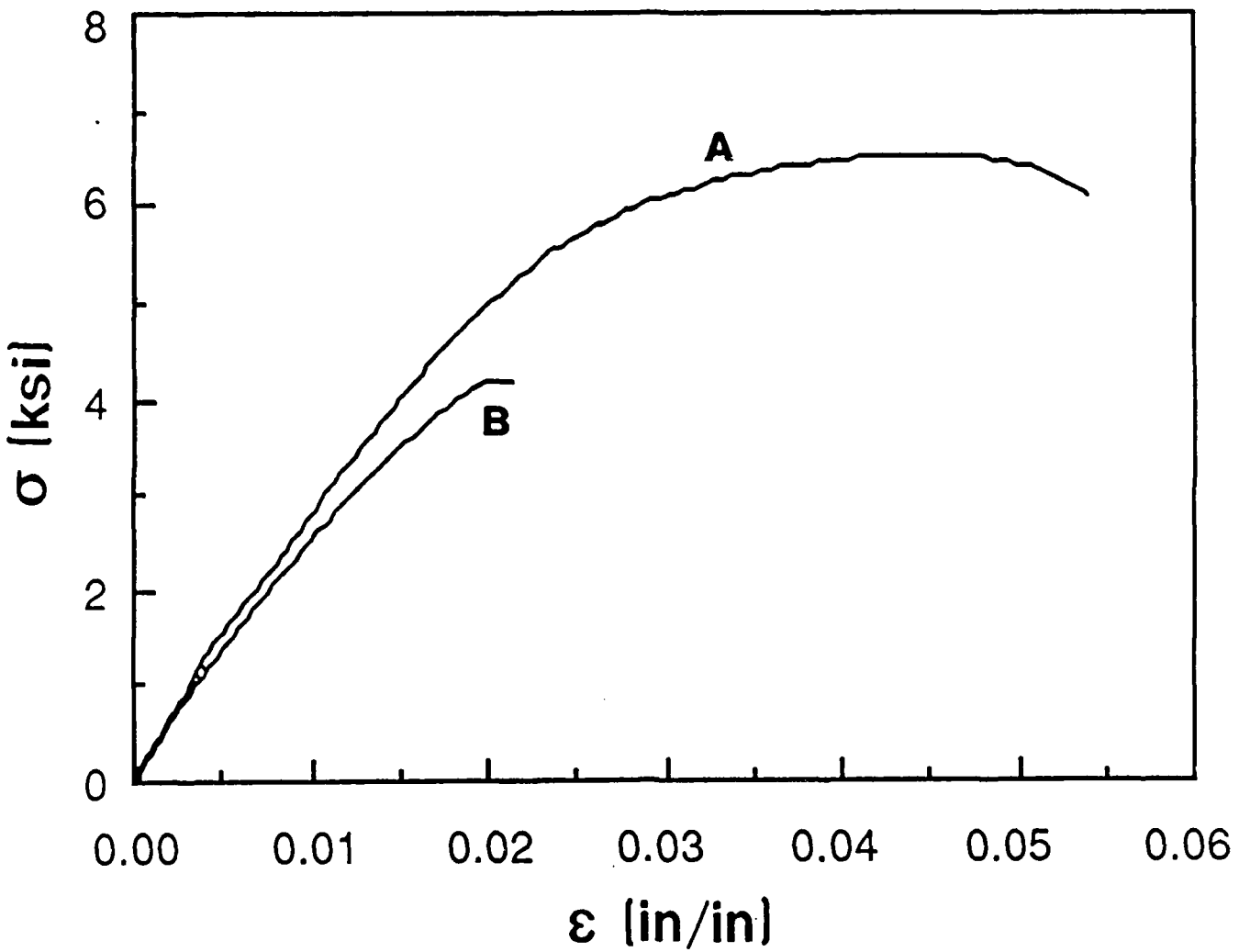

Figure 23. Stress-strain behavior of (A) Epon 828/1SA and (B) blend material. The blend fractured at a void.

4. COMPOSITES, AND FIBER AND INTERLAMINAR COATINGS

4.1 Experimental

Composites

In an attempt to produce samples more or less representative of the potential use of C8 as a matrix for composites, samples consisting of ca. 50% graphite fibers were prepared. AS4 fibers were layed unidirectionally by hand in silcone molds of a dogbone shape, 2.5×0.5×1/8 inch with 1.5×0.25 inch gauge. The C8/1SA resin was poured into the mold and fully cured using the standard curing cycle. The resin "wet out" the fibers well.

Aging histories were removed from composite specimens by annealing at 120°C for 1/2 hour just prior to testing. These samples were tested in tension using the Instron 1331 set up described above.

One of the samples that failed to break in tension was fractured in flexure. One of these fracture surfaces was polished and ion etched for 20 min. in an air plasma. Both surfaces were coated with Au-Pd and examined using the Hitachi S570 SEM discussed previously. The etched sample was examined at a working distance of 13 mm. while the shear fracture surface was examined at a working distance of 30 mm. to obtain a greater depth of field.

Interlaminar Coating

Two pieces of a non-postcured Epon 8280/V40 material in standard dogbone shape were obtained from W.-T. Chen. The surfaces were coated with C8/1SA which had been mixed for 30 min at 55°C. The coating was outgassed for 20 min under vacuum, at which point the two surfaces were pressed together. The laminated sample was then cured for 16 hours at room temperature followed by a 3 hour postcure at 120°C. The laminate was fractured in shear. One surface was etched for 15 min. in an air plasma. Both surfaces were coated with Au-Pd and investigated in the SEM with a 13 mm. working distance.

Single Fiber Tests

Dogbone samples were molded in two part molds. The lower cavity was 1/8 inch deep. Several fibers were carefully laid across the cavity longitudinally. A second dog bone mold of over 1/4 inch thickness was placed over the lower mold to hold the fibers in place. The second layer was open to the air to enable filling and outgassing of the samples. After curing the sample, excess material above the surface was mechanically removed for a total specimen thickness of 1/4 inch. The surfaces were polished optically smooth with 0.3 micron alumina powder. Specimen aging histories were removed and the sample was examined optically to determine the condition of the fiber.

Two varieties of sample were fashioned. The first type was an Epon 828/1SA matrix (cured in the same manner as the C8 resin is cured) with AS4 fibers. The second sample type also had an Epon 828/1SA matrix, but the fibers were AS4 coated with C8/1SA.

The coated fibers were prepared as follows: AS4 fibers were laid across a wire rack and glued in place. C8/1SA resin was mixed in stoichiometric proportions and mixed for 30 min at 60°C. The reaction mixture was then diluted 12:1 with acetone and poured over the fibers. These fibers were then dried under vacuum at 30°C

The aging histories of these two sample types were removed before examination under tension on a tensile stage attached to a Reichert Zetopan optical microscope. The formation of the birefringence was recorded photographically. Tension was released and the critical lengths of the broken fibers were measured using a combination of bright field and birefringence patterns to locate break points.

4.2 Results and Discussion

Composites

The mechanical properties of the composite are shown in Figure 24. The shape is somewhat unusual, initially concave upwards followed by a change to more normal elastic behavior at .35% strain. The composite was also impossible to break

in tension. No matter what the circumstances the material would fail, breaking up into many pieces in the grips, while the run proceded. Thus, the upper point in the figure does not represent the ultimate failure strength of the composite. This behavior has been noted in other instances in this lab when unidirectional composites have been tested. Apparently the unidirectional composite is very unstable in the transverse direction. Failure measurements have been obtained in these cases by gluing metal tabs to the ends to improve the dimensional stability within the grips. Such measurements have not been completed as yet.

The concave nature of the initial behavior is attributed to the initial stress being supported by a reduced number of fibers, the number increasing as the fibers straighten. The initial modulus of 16×10^3 ksi is very close to the theoretical va e (by the rule of mixtures) of 16.6×10^3 ksi, suggesting that most of the fibers are straight to begin with.

Low magnification EM of the polished and etched surface (Figure 25) show the layup of the fibers and the matrix disruption characteristic of the fluoroepoxy when exposed to the ion etching process. The higher magnification in Figure 26 is consistant with the ion etching observations, but even under these adverse conditions material can be found adhering to many of the fibers.

The flexure failure surface micrographs (Figures 27 and 28) also exhibit evidence of good adhesion. In Figure 27a

the fibers have been pulled from the matrix, while in b the fibers are protruding to such an extent that even at the large working distance the ends are out of focus. The arrows point to fluoroepoxy adhering to the surfaces of the fibers. The arrow in Figure 28 points to a place where large quantities of fluoroepoxy are adhering to and binding two fibers together.

Yet if adhesion is so good, why is there so much fiber pull-out? For perfect adhesion one would normally expect the fracture plane to proceed straight through the matrix and fibers. We note, however, that the fractured specimen had already undergone a tensile test. It is likely that during the tensile test the fiber fractured at points randomly throught the gauge region and then debonded along the fibers due to interfacial shear. Upon flexure, these fibers would appear to "pull out" as the fracture propagated. The microscopic work indicates that C8/1SA adheres well to the AS4 fibers that pulled out.

Interlaminar Ply Coating

Figure 29 shows the interface of two plys of Epon 8280/V40 glued with C8/1SA after undergoing flexural fracture at room temperature. Obviously, failure did not occur perpendicular to the "glue" line but rather propagated along or in the glue line for a considerable distance. We suggest failure is occurring in the C8 layer, close to the interface. Arrow (a) indicates a point where fracture

proceeded through the interlayer as well as along the interfaces, while arrow (b) indicates a region which we believe consists of a film of fluoroepoxy adhering to the Epon. In Figure 30, the ion etched version of Figure 29, one sees that some of the fluoroepoxy appears to still be adhering to the Epon layer. Hence, a moderately strong interface for the coating is tentatively suggested.

Single Fiber Tests

Single fiber tests are currently in an embryonic state. The initial results look promising, but to date all samples investigated have been formed using the silicone mold releases used in the other tests. The mold release agent might contaminate the fiber surfaces, having an unknown effect on the results, which are thus in need of confirmation using additional samples.

The critical lengths of the two systems are detailed in Table 5. The critical length of the coated fibers is significantly smaller. Assuming the ultimate fiber strengths to be the same in both cases, this translates to a stronger interfacial strength.

In Figure 31 the development of the birefringence as tension is applied is illustrated. Figure 31A shows the initial shape of the birefringence just as the initial breaks in the fiber are formed (indicated by the arrows). In figure 31B, the leftmost fiber break has moved out of the field to the left, while another break has occurred

(indicated by the arrow slightly left of center). The birefringence pattern is also noted to begin to localize, becoming closer to the fiber. Drzal[19] has indicated that this is due to the progress of fiber debonding, or in this case to debonding of the matrix and fiber coating. On the other hand, the C8 coating, in its non-aged state, is much more compliant than the matrix, perhaps concentrating the strain in a narrow sheath close to the fiber. In figure 31C the birefringence narrows more, retaining its diffuse nature only at the low strain nodes between breaks. No further breaks have occurred, indicating that the strain at which the fiber breaks apart into critical lengths had been exceeded. In figure 31D the sample is approaching failure. The birefringence has gotten very narrow, and in places where the fiber has slipped there are long stretches of low birefringence where the strain has relaxed. An asymmetry has also formed in the birefringence slightly to the right of the break indicated by the left arrow. The formation of this asymmetry at deformations close to matrix failure has been suggested by Drzal[19] to be due to shear banding type failure of the matrix induced locally by the fiber.

Figure 32 shows a different area of the same sample after failure has allowed the stress to relax. Arrow a indicates a region where the fiber slipped while in tension, causing a kink in the fiber where the ends compress after meeting during relaxation. Arrow b indicates a more normal birefringence pattern occurring at fiber breaks. The

asymmetric shadow indicated by arrow c is a remnant of the matrix failure by such mechanisms as shear banding.

Figure 33 is an optical montage of the birefringence along an uncoated fiber in an Epon 828/1SA matrix under tension. The large amount of asymmetry in the pattern could be due to matrix failure, as before, or, as is suggested by the regularity of the distortions, could be due to localized debonding (or, equally, localized adhesion) of the fiber and matrix. Note that the overall pattern is more diffuse than that seen in the coated fiber specimen, indicating a broader area of deformation. The lighting change from left to right in each photograph is an artifact of the microscope used.

Tears were seen in both of the samples prior to straining. According to Drzal[19], these are called diamond flaws and are caused by the shrinking of the matrix during crosslinking. The fiber causes the stresses of this process to localize and form the flaws.

To take full advantage of the single fiber tests, care must be taken not to greatly exceed the minimum strain necessary to break the fiber apart into its critical lengths. Microtoming along the fiber can also be used to determine whether fracture is occurring or if material adheres to the fiber. These experimental refinements, as well as limiting the use of release agents, have yet to be performed.

4.3 Conclusions

SEM studies of the unidirectional composite showed that there is excellent adhesion of matrix to fiber and that the load transfer, at least to the rough approximation of the rule of mixtures, enables nearly the maximum obtainable modulus. Aging effects and low T_g, however, reduce the value of the C8 resin as a matrix material.

The lamina coating of two plys of Epon 8280/V40 was less successful. While there is some evidence for adhesion, it is not really conclusive.

The single fiber tests are interesting, exhibiting many features that are of potential use. The only clear results from the tests, however, were the critical lengths of the uncoated and C8/1SA coated fibers in an Epon 828/1SA matrix. These suggest that, using C8/1SA as a model, the fluoroepoxies can be successfully employed as fiber coatings with the potential for both preventing the infiltration of moisture along the fibers and improving the interfacial shear strength of materials employing them. Further tests of this nature may be justified.

Our results using C8/1SA as a model system indicate that the fluoroepoxies have excellent potential as components in composite materials for naval appplications. As a result of the studies described above, work is currently underway by Griffith on synthesis of materials with both

higher T_gs (for structural materials) and lower T_gs (for use in blends).

Table 5. Critical lengths of fibers in single fiber tests.

Matrix	Fiber	ℓ_c
Epon 828/1SA	AS4	1.0±0.4 mm
Epon 828/1SA	AS4/C8/1SA	0.5±0.2 mm

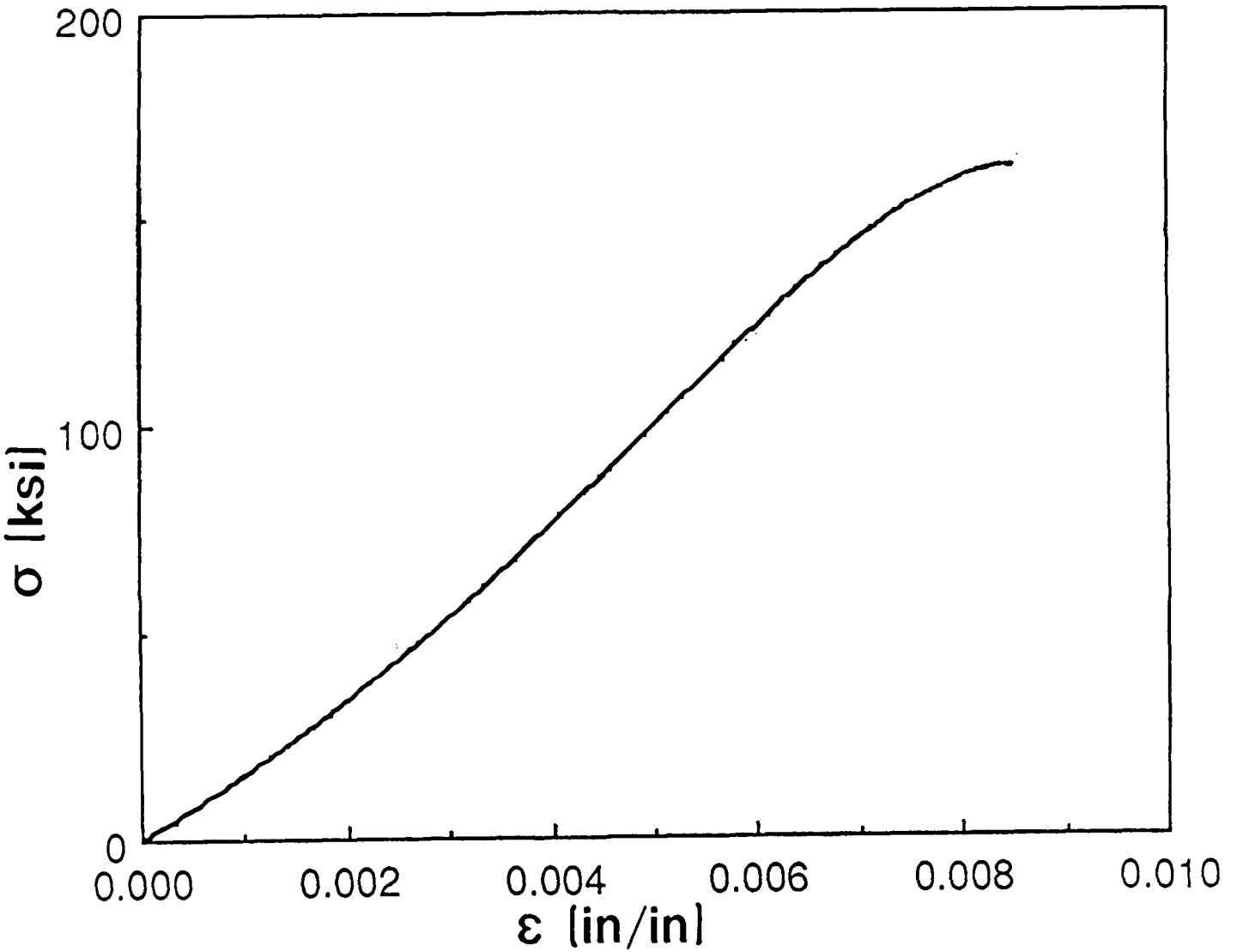

Figure 24. Stress-strain behavior of C8/1SA-AS4 unidirectional composite under tension. Crushing in the grips forced premature termination of the test.

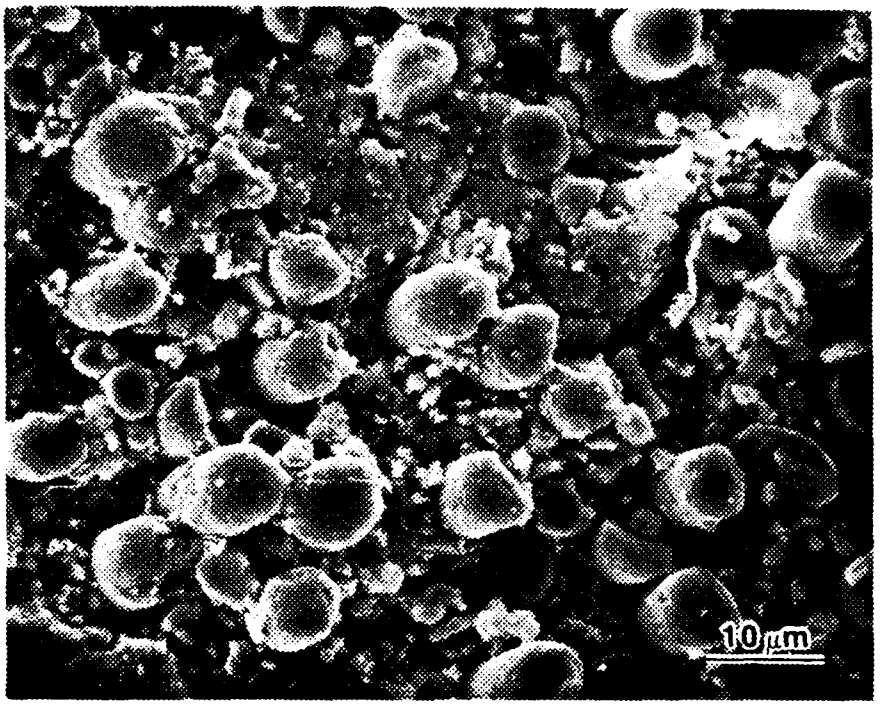

Figure 25. Low magnification SEM of a fractured, polished and etched composite sample. Notice the disrupted nature of the matrix due to etching. Note also the more or less random fiber packing.

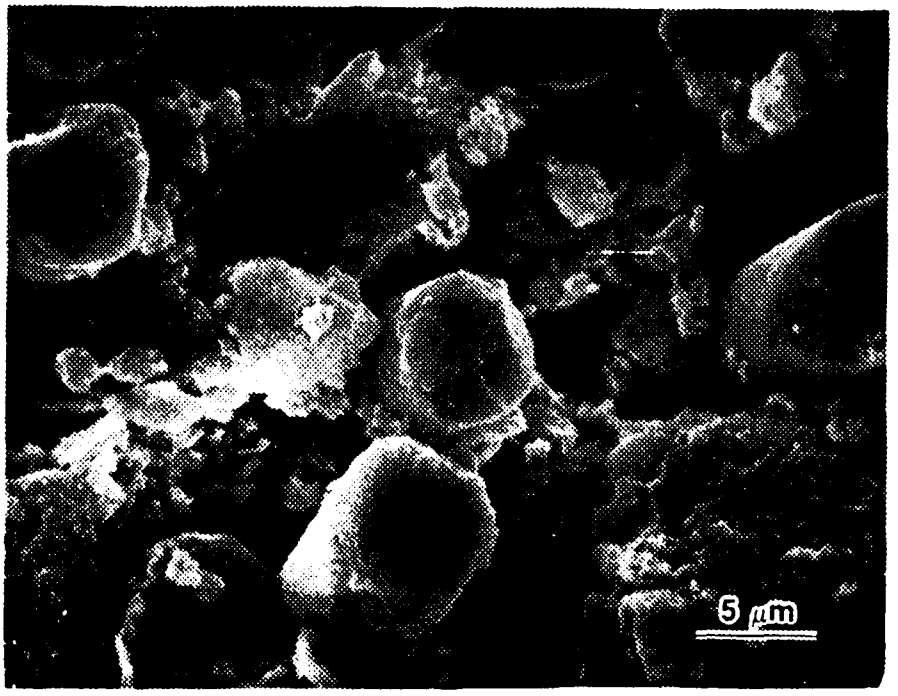

Figure 26. Higher magnification of Figure 25. Notice that some material seems to be adhering to the fibers, even after etching.

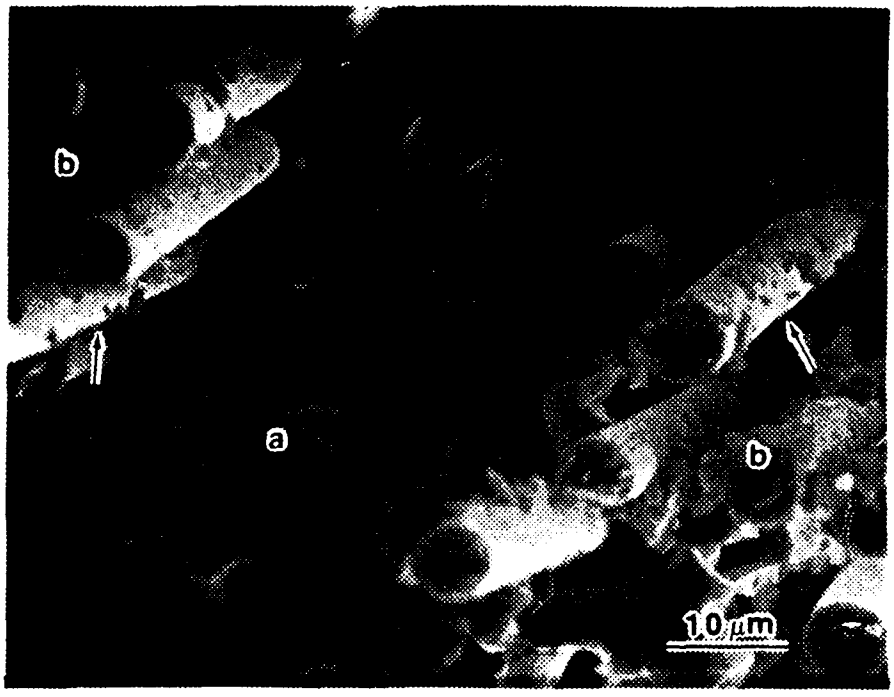

Figure 27. Micrograph of a flexurally fractured composite surface. Notice the length of fibers exceeding the depth of field. (a) holes where fibers have pulled out, (b) fibers that have pulled out of the other surface. The arrows point to material adhering to the fibers.

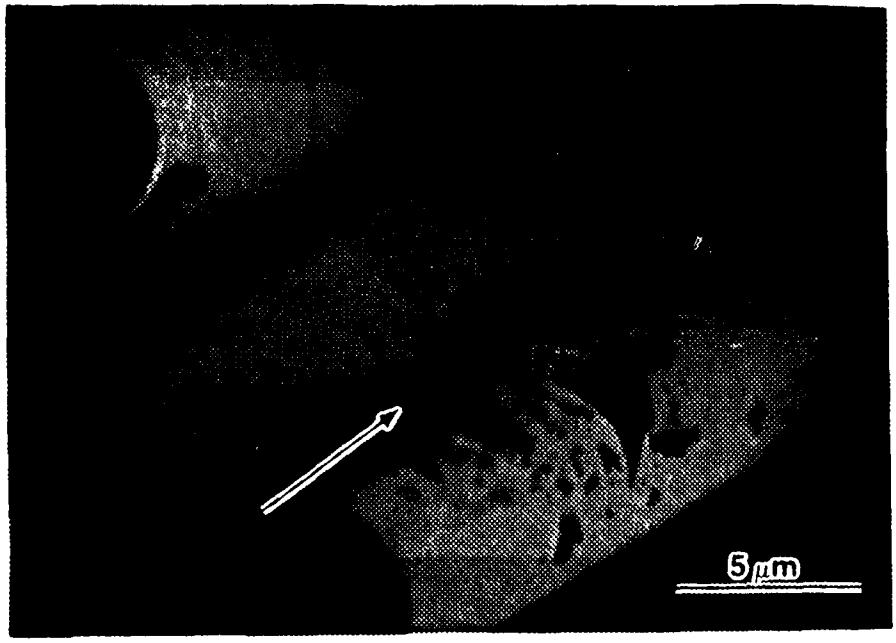

Figure 28. Magnified image of a cluster of fibers from the flexure fracture pictured above. The arrow points along the interface between two fibers, where a large quantity of fluoroepoxy is adhering.

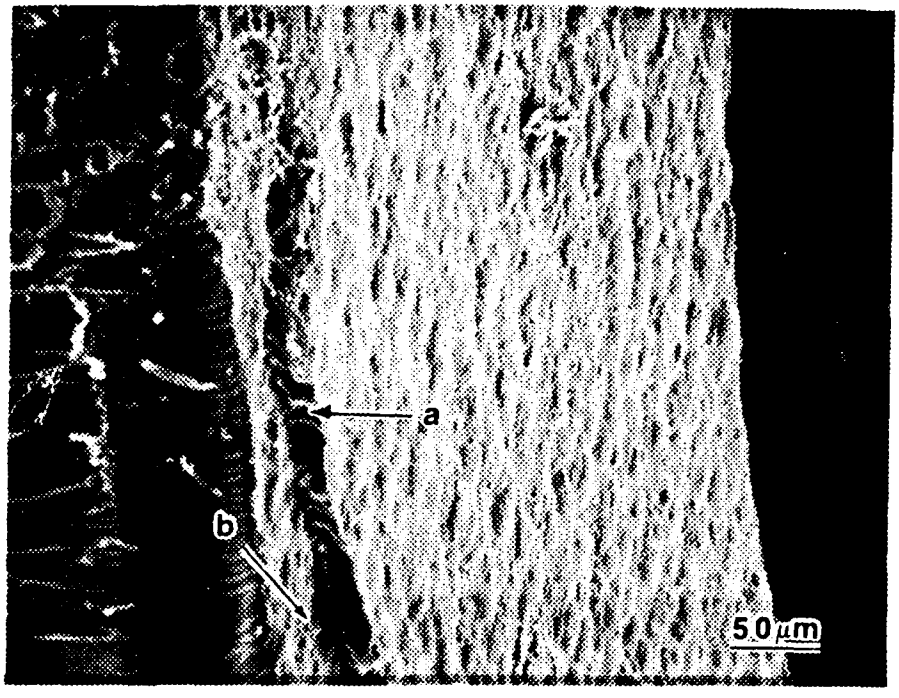

Figure 29. SEM of the flexural fracture surface of two plys of Epon 8280/V40 laminated with an interlayer of C8/1SA resin. (a) points to a point where it is suggested that failure occurs in the coating. (b) points to a film of fluoroepoxy adhering to the surface.

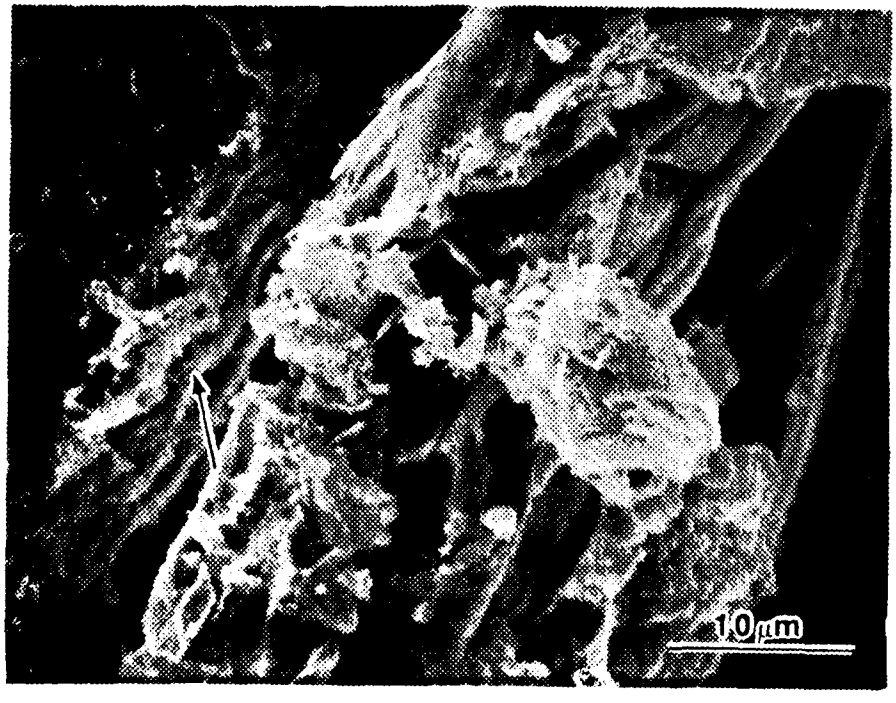

Figure 30. SEM of an etched version of the sample in Figure 29. The arrow points to fluoroepoxy adhering to the ply surface.

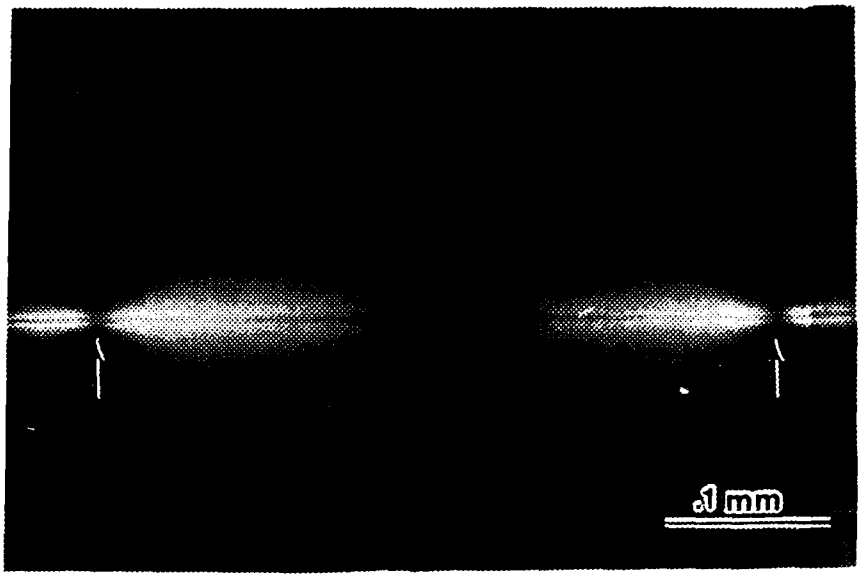

A

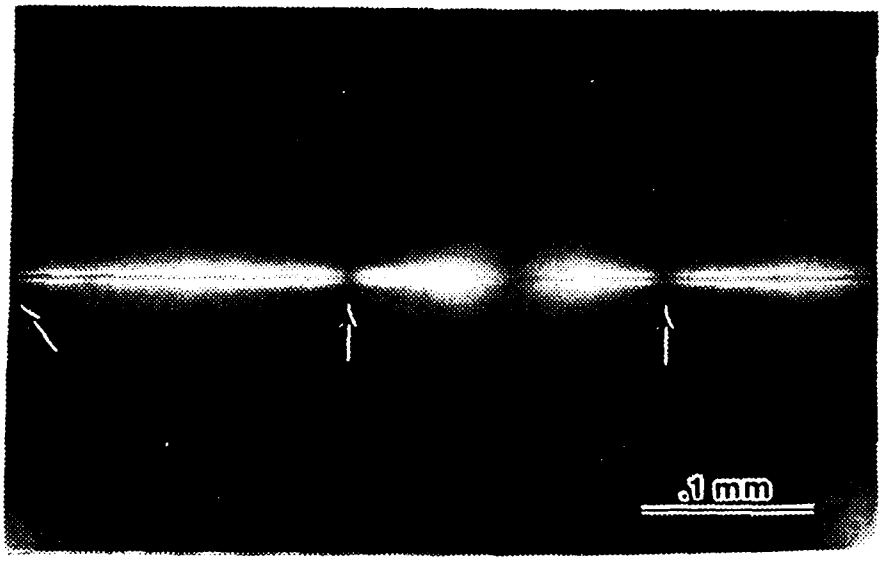

B

Figure 41. Optical micrographs of the development of the stress birefringence around the coated fiber. (a) initial formation, two breaks indicated by arrows. (b) another break has occurred, but one break has moved out of the field. (c) the distance between breaks is growing. (d) final pattern before failure.

C

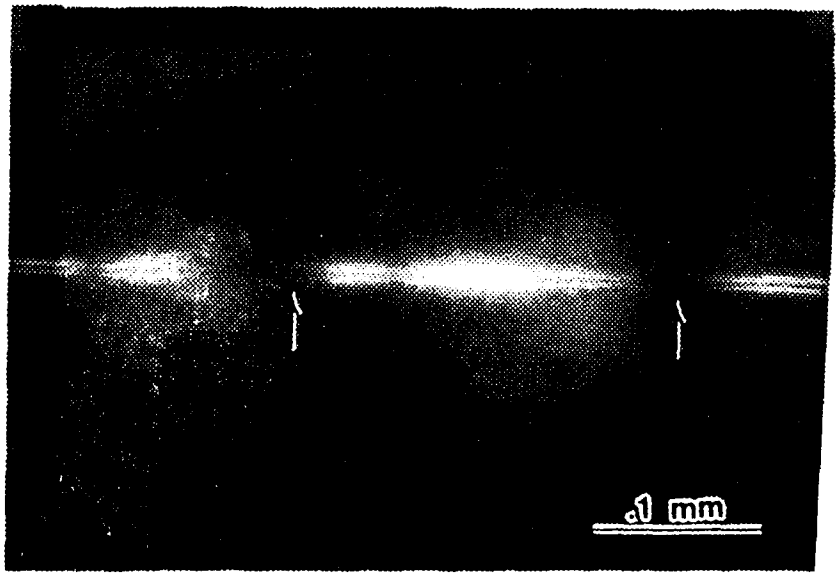

D

Figure 31. (Continued) Optical micrographs of the development of the stress birefringence around the coated fiber.

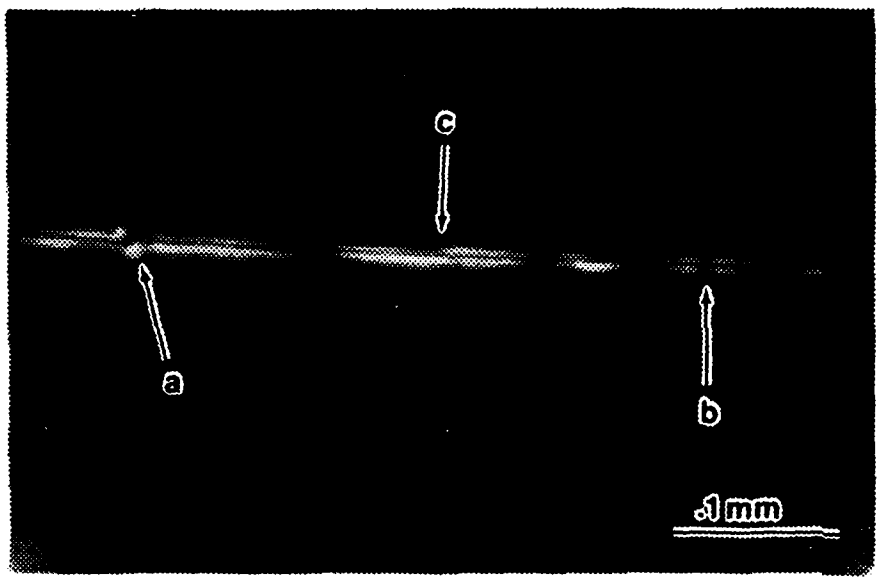

Figure 32. Optical micrograph of a different area in the above sample after fracture. (a) kink where the fiber has slipped and then compressed. (b) normal break. (c) angled birefringence shadow of unclear origin (see text).

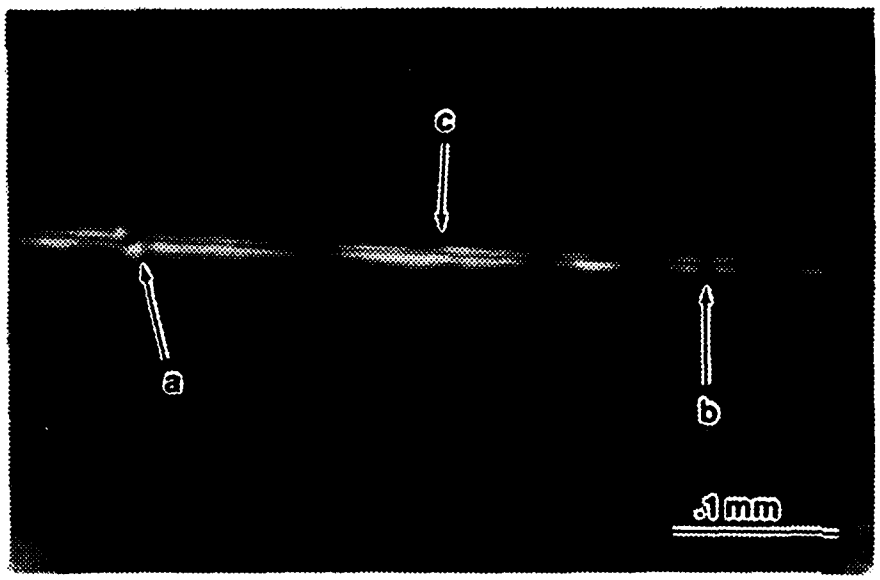

Figure 32. Optical micrograph of a different area in the above sample after fracture. (a) kink where the fiber has slipped and then compressed. (b) normal break. (c) angled birefringence shadow of unclear origin (see text).

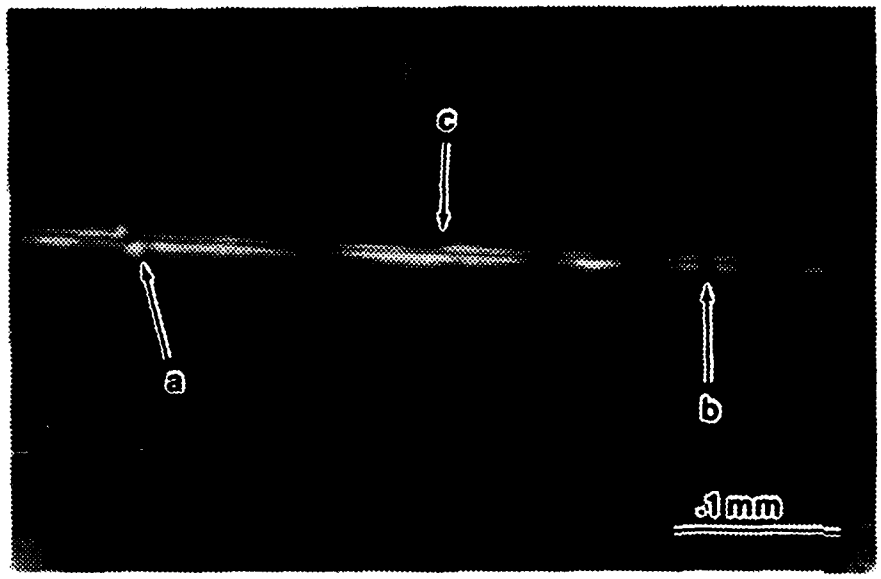

Figure 32. Optical micrograph of a different area in the above sample after fracture. (a) kink where the fiber has slipped and then compressed. (b) normal break. (c) angled birefringence shadow of unclear origin (see text).

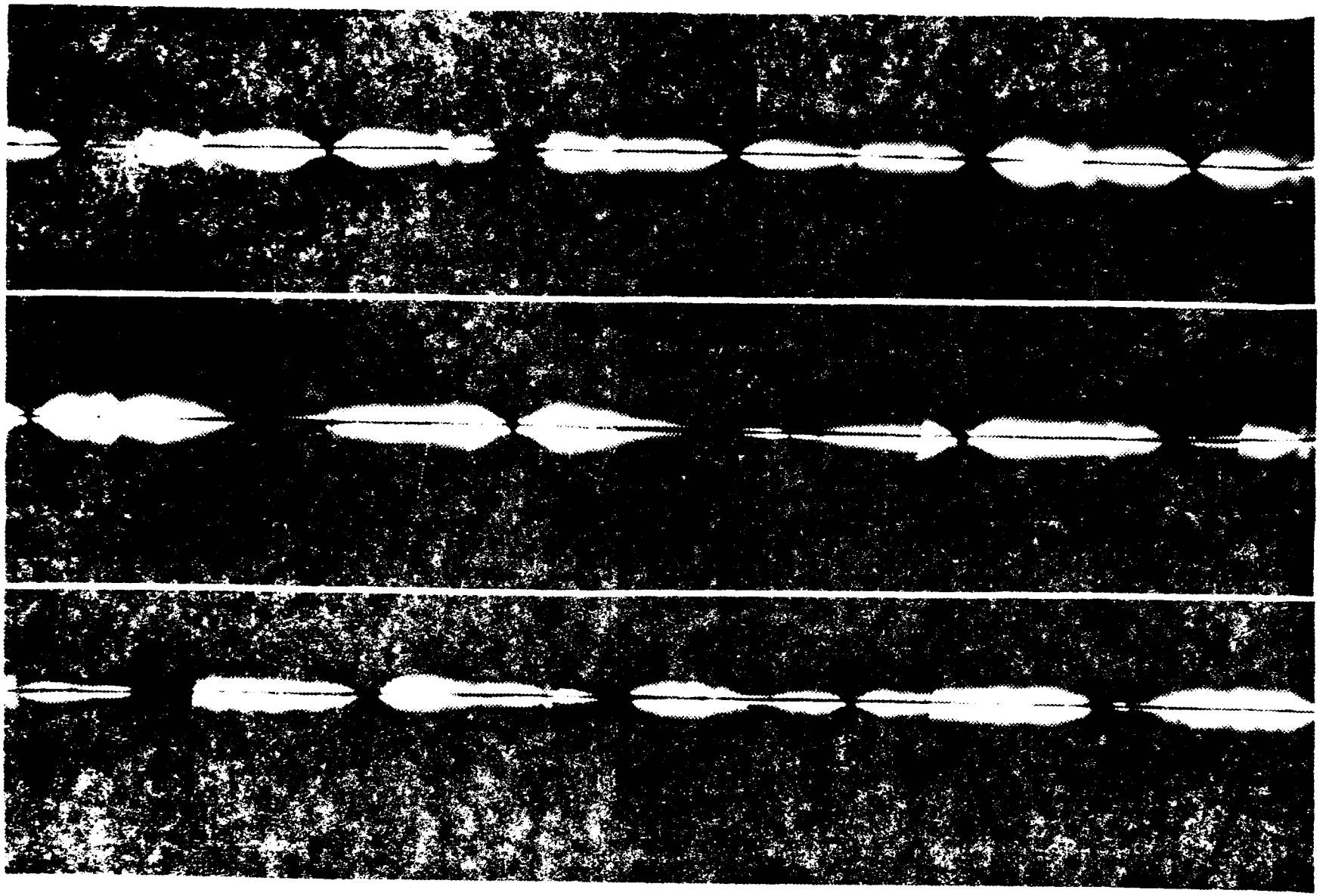

...ical ... image along an uncoated AS4 fiber in ... fiber 828 matrix illustrating various stress ...ringence features (see text).

5. CONCLUSIONS

Structural Considerations

The neat resin has been characterized in terms of its relaxation behavior as a function of cure and in respect to some of its physical properties. While the mechanical properties found were reasonable, the material undergoes a radical change in properties not far above room temperature. Cure requires special considerations to avoid the absorbtion of CO_2 with commensurate crystallization of unreacted hardener. The material also ages rapidly at room temperature, changing from a ductile to a brittle material in a matter of months. All of this is strong recommendation against the pure resin as a structural material.

The C8 resin was blended 10% by weight with Epon 828 and cured with 1SA. This material exhibited Epon dominated mechanical behavior. XPS shows that the fluoroepoxy goes selectively to the upper surface of the mold, providing a process controlled method for interply layers in laminates. Microscopy indicates spherical domains arising from the fundamental incompatability of the two resins. These domains incorporate the potential for a toughened material. The material welds well, with no defects visible in SEM studies. This model system indicates that a potentially successful fluoroepoxy containing self toughened material

(with both toughening domains and interply layers can be produced during processing.

Unidirectional composites and single fiber tests strongly indicate very good adhesion between fluoroepoxy and fiber. This strength has also been found to be transferred to a more standard resin matrix through fiber coating. The use of fluoroepoxy to coat plys in lamination was less successful, but not completely without hope.

The fluoroepoxy, however, maintains some weaknesses which have not be surmounted. The aging of the fluoropolymer will affect the behavior of blend and composite adhesion in an unknown but surely detrimental fashion. Also, all the room temperature properties will change radically when the temperature is raised just 10 to 15 degrees. So, while the composites, blends and coatings hold promise, they hold challenge as well.

Griffith, as was mentioned previously, is currently working on systems to answer these challenges. He is making materials with both subambient T_g for use in rubber toughening blends and higher T_g for possible composite applications. Either will solve the aging problem, aging being less of a problem for high T_g material and not occurring for low T_g materials.

Up until this point, no mention has been made of the relatively long curing times used and their application to processing. The long pot life lends itself well to long filament winding processes. With proper application of heat

or other catalysis or inhibitors and diluent, the pot life can potentially be changed as desired for other processes.

REFERENCES

1. C. E. Browning, Polym. Eng. Sci., 18, 16, 1978.
2. E. L. McKague, J. D. Reynolds and J. E. Halkais, J. Appl. Polym. Sci., 22, 1643, 1978.
3. M. K. Antoon and J. L. Koenig, J. Macro. Sci.-Rev. Macro. Chem., C19, 135, 1980.
4. W. C. Wake, "Adhesion and the Formulation of Adhesives", Applied Science, 1976.
5. J. R. Griffith and D. E. Field, Report on NRL Progress, June 1973.
6. J. R. Griffith, Chemtech, 12, 290, 1982.
7. J. R. Griffith, S. A. Reines and J. G. O'Rear, NRL Report 7127, August 19, 1970.
8. D. L. Hunston, J. R. Griffith and R. C. Bowers, ACS Ind. Eng. Chem. Prod. Res. Dev., 17, 1, 1978.
9. S. J. Shaw, D. A. Tod and J. R. Griffith, Polymer Preprints, 1986.
10. S. J. Shaw, Personal Communication, 1987.
11. E. A. Turi (ed.), Thermal Characterization of Polymeric Materials, Academic Press, 1981.
12. S. Pangrle, C. S. Wu and P. H. Geil, Report No. UILU-ENG-87-5015 (University of Illinois), 1987.
13. J. van Turnhout, "Thermally Stimulated Discharge of Polymer Electrets", Elsevier, 1975.
14. W. D. Bascom and R. M. Jensen, J. Adhesion, 0, 1986.
15. L. T. Drzal, M. J. Rich and P. F. Lloyd, J. Adhesion 16, 1, 1982.
16. M. B. Munro, A. Miyase, R. C. Flanagan, D. Lindstrom, D. Bouchard, C. Aleong and J. Wong, Report No. UOME-FP-8304-1 (University of Ottawa), 1983.
17. J. R. Griffith, Personal Communication, 1988.
18. C. D. Wagner, W. M. Riggs, L. E. Davis, J. F. Moulder and G. E. Muilenberg (ed.), "Φ Handbook of X-Ray Photoelectron Spectroscopy", Perkin-Elmer Corporation, 1979.
19. L. T. Drzal, Personal Communication, 1988.

ACKNOWLEDGEMENTS

This research was supported by the Office of Naval Research through the University of Illinois National Center for Composite Materials Research. T. E. Twardowski also acknowledges receipt of a ONR-URI fellowship.